A Multi-Criterian Approach to Identify Groundwater Potential Zones in the Subarnarekha River Basin UsingIntegrated AHP and Geospatial Technology

Abstract

The intense extraction of groundwater and changing climate patterns have strained global groundwater supplies. As the demand for drinkable water rises worldwide, assessing groundwater availability and aquifer output becomes increasingly important. Geographic information systems (GIS) are being used more frequently for groundwater exploration due to their speed and provision of preliminary data. This study focuses on mapping groundwater availability in a minor tropical river basin in India, using a combination of GIS and the analytical hierarchy process (AHP).Ten thematic layers were generated and analyzed, including Geology, Geomorphology, LULC, Lineament density, Drainage density, Rainfall, Soil, Slope, TWI, and Curvatureto delineate groundwater potential zones. AHP was employed to assign weights to each category based on their water retention properties.The resulting map was validated against existing groundwater data, demonstrating an accuracy of approximately 85%. The groundwater potential zones were classified as high, moderate, and, low. The moderate potential zone covered 59% of the basin, while the low and high potential zones constituted 29% and 11% respectively. High and low potential regions were limited to small sections of the basin.In conclusion, this research successfully mapped the groundwater availability in the RarhuRiver watershed using GIS and AHP. The findings highlight the distribution of different groundwater potential zones, providing valuable information for sustainable water resource management in the area.

Keywords: Groundwater potential zone; Analytical hierarchy process (AHP); Multi-criteria decision analysis (MCDA); Remote sensing and GIS; Rarhu watershed

1. Introduction

Water is the foundation of ecosystems and the essential ingredient for life itself. In addition to being essential to human life, water is also a priceless gift for all plants, animals, and other living things National Water Policy 2002. This priceless resource kindly supplies about 34% of the freshwater needed to support human civilization worldwide (Dar et al. 2010; Ghosh et al. 2016; Murmu et al.2019). In India, 50% of the urban and 90% of the rural populations get their domestic water from groundwater. In addition, the agricultural sector uses around 70% of the groundwater in the nation (Dhawan, 2017). There are two main sources of water: sub-surface water, also called groundwater, which appears as springs, wells, infiltration wells, and galleries, and surface water, which includes rainwater, river water, lake water, and ocean. Because of its chemical makeup, constancy in temperature, purity, and reduced contamination susceptibility, groundwater is vital to towns, industry, and agriculture worldwide.Numerous natural and man-made variables influence the distribution and availability of groundwater, with tropical and subtropical areas experiencing major issues due to high population density and economic activity. According to the NITI Aayog, the lack of freshwater availability in India puts about 0.6 million people under high to extreme water stress. The seriousness of the problem is further demonstrated by the fact that 75% of Indian households do not have access to clean water on their property. The World Bank has issued a concerning report indicating that without immediate

action, India will confront a severe water crisis in the upcoming decades. It's projected that by 2025, the nation will experience water stress, with the possibility of becoming a water-scarce region by 2050 (IWE2006). Groundwater, presently contributing 34% to India's annual water supply, demands meticulous management to stave off this impending crisis. Fortunately, the utilization of geographic information systems (GIS) and remote sensing technologies present robust solutions for the monitoring and management of this essential natural resource (Dar et al.2010; Magesh et al 2012).Traditional methods for identifying and mapping regions with substantial groundwater potential heavily rely on comprehensive ground surveys utilizing geophysical, geological, and hydrogeological techniques. However, these approaches tend to be costly and time-intensive (Changnon et al.1988; Israil et al., 2006; Ashoka et al., 2018). Conversely, geospatial instruments present a swifter and more economical approach to generating and simulating crucial data across diverse geoscience fields. These instruments offer an efficient substitute for evaluating zones of groundwater potential (Ganapuram et al., 2009; Adiat et al., 2012; Moghaddam et al., 2015; Russo et al., 2015).

A review of existing literature demonstrates the diverse array of methods researchers have employed to identify and map groundwater potential zones. These techniques include probabilistic models like Shannon's entropy, decision trees, artificial neural networks, weights-of-evidence, logistic regression, evidential belief function, certainty factor, and frequency ratio. They also include machine learning techniques like random forest and maximum entropy modeling. (Corsini et al., 2009; Ozdemir 2011; Lee et al., 2012; Mukherjee et al., 2013;Nampak et al., 2014; Rahmati et al., 2015; Pourghasemi et al., 2015; Pourtaghi et al., 2014; Naghibi et al., 2015; Razandi et al., 2015; Mogaji et al., 2015). Notably, remote sensing and geographic information systems (GIS) emerge as particularly potent tools for swiftly estimating the potential and distribution of natural resources. The integration of these geospatial

technologies offers an efficient approach to assessing groundwater resources across extensive areas before conducting costly surveys (Faust et al., 1991; Hinton and J.C 1996; Jha et al., 2007).

In this investigation, we utilized a combined strategy, integrating the MCDM, Analytical Hierarchy Process (AHP), and, Geospatial techniques, toward outline groundwater potential mapping. AHP, introduced by Tomas Saaty in 1980, proves invaluable for tackling intricate decision-making in groundwater-related domains. This methodology simplifies complex decisions by conducting pairwise comparisons and then consolidating the findings. Moreover, AHP incorporates a feature designed to evaluate outcome consistency, hence mitigating decision-making bias. Througha fusion of AHP and GIS capabilities, this approach offers a robust method for mapping and evaluating regions with substantial groundwater potential (Saaty and T.L. 1990). The study centered on the Rarhu watershed, a small tributary of the Subarnarekha River originating in the northeastern part of the Ranchi plateau. The Rarhu River, draining this northeastern plateau region, serves as a crucial lifeline for a large population heavily reliant on agriculture. Groundwater supplies are vital to the communities in this area for household, agricultural, and horticultural uses.

The foremost aim ofthis research was to demarcate, classify, and mapping of the groundwater potential zones within the Rarhu watershed. The goal of this project was to present a case study that may serve as a model for the development of sustainable water resources and regional planning techniques. By accurately assessing and mapping areas with high groundwater potential, the findings can guide efforts toward prudent management and utilization of this vital resource, thereby bolstering water security and sustaining the livelihoods of the local populace.

1.1.Study Area

The study zone encompasses the Rarhu watershed, a significant right-bank tributary within the Subarnarekha River system. Positioned in the eastern part of peninsular India, it lies southeast of the Chotanagpur plateau within the Ranchi district of Jharkhand state. Covering an area of roughly 600.53 km^2 in the drainage basin of Subarnarekha, the Rarhu watershed spans latitudes 23°27'6.962" N to 23°12'56.651" N and longitudes 85°23'11.79" E to 85°51'37.613" E (Fig. 1). The highest elevation reaches 777 meters above mean sea level. Originating from Baram village in the Namkum community development block of Ranchi district, the Rarhu River stretches approximately 56.11 km^2 merging with the Subarnarekha River near Shyam Nagar in the Birdidih area of West Bengal at an elevation of 152 meters (Fig. 2). This watershed serves as a significant case study area for evaluating groundwater potential and formulating sustainable water resource management strategies for the region.

2. Materials and Methods

To identify groundwater potential zones within the Rarhu watershed, this study used geospatial techniques. Following a comprehensive review of global and regional literature, ten thematic layers were selected for identifying groundwater potential zones (Table 1).Ten thematic data layers encompassing the region's geology, geomorphology, land use/land cover (LULC), drainage density, lineaments, rainfall, soil, slope, curvature, and topographic wetness index were integrated using a knowledge-based factor analysis technique(Table 2). Remote sensing data preprocessing for the Rarhu watershed was conducted using ERDAS Imagine 2015 image processing software. Geographic Information System (GIS) techniques were applied using ArcGIS 10.7.1. Topographic map sheets at

a 1:50,000 scale from the Survey of India (SOI 73E/11, 73E/15, 73E/16) were employed to delineate the watershed boundary and calculate drainage density and lineament density. Sentinel 2A satellite imagery with a spatial resolution of 10m, specifically a geo-coded false-color composite (FCC), was utilized to generate LULC thematic layers within the GIS framework (Dar et al. 2010).

The amalgamation of various geospatial datasets and analytical methodologies empowered researchers to systematically assess and map areas demonstrating high groundwater potential within the Rarhu watershed. Existing maps illustrating the geology, geomorphology, and soil attributes of the region were sourced from the Bhukosh and FOA soil portals, digitized, and tailored to fit the study area boundaries. Terrain parameters such as slope, curvature, and topographic wetness index (TWI) were extracted from high-resolution digital elevation model ALOS PALSAR (12.5m) data (Magesh et al., 2012; Kumar et al., 2016).

Rainfall data for the area was retrieved from the IMD Pune data portal. Using the inverse distance weighting (IDW) interpolation method, a geographical distribution map of the watershed's rainfall patterns was created (Arulbalaji et al., 2016; Nair et al., 2017). Through the synthesis of this diverse array of geospatial data layers about various environmental factors, the researchers conducted a comprehensive analysis to delineate zones showcasing promising groundwater potential within the Rarhu watershed.

2.1.Multi-criteria decision analysis (MCDA) using GIS techniques.

One well-known GIS-based multi-criteria decision analysis technique for defining groundwater potential zones is the Analytical Hierarchical Process (AHP). This technique facilitates the amalgamation of various thematic data layers that influence the occurrence and movement of groundwater. In this study, a total of 10 distinct thematic layers were assessed, representing factors governing water

flow and storage within the area of interest. The significance and interrelationship of these influencing factors were quantified through assigned weights, reflecting their expected contributions to groundwater occurrence and expert judgment. Parameters with greater weights indicate a more significant impact on groundwater potential, while those with lower weights suggest a lesser influence. The precise weights allocated to every characteristic were ascertained by using Saaty's basic relative importance scale, which spans from 1 to 9. The researchers' expertise in the field of study and a thorough analysis of earlier, pertinent studies served as the foundation for this weight-assigning process.

By combining the ten weighted theme layers via the AHP multi-criteria analysis framework, the researchers synthesized diverse spatial data to delineate areas demonstrating relatively higher potential for groundwater resources.A value of 9 indicates extreme importance, 8 indicates very strong importance, 7 indicates very strong to extreme importance, 6 indicates strong plus importance, 5 indicates strong importance, 4 reflects moderate plus importance, 3 indicates moderate importance, 2 indicates weak importance, and 1 indicates equal importance. Saaty's basic scale of relative importance provides a quantitative framework for allocating weights. The thematic layers were given weights according to their prospective water-holding capacity and perceived value using this classification.

To determine these weights, pairwise comparisons were conducted for all thematic layers, resulting in a comparison matrix (Table3).After the initial pairwise comparison of thematic layers, the judgment matrix underwent normalization. Next, the consistency index (CI) and the random consistency index (RI) were calculated. The principal eigenvalue (λmax) was derived, enabling the computation of the consistency ratio (CR). The final weights allocated to each thematic layer were determined based on the CR value less the 0.1,

which evaluates the consistency of pairwise judgments throughout the Analytical Hierarchy Process (Table 4).Within the GIS platform, the sub-classes of each thematic layer underwent reclassification using the natural breaks classification method. These sub-classes were then ranked on a scale from 0 to 9, representing their relative influence on groundwater development and occurrence. This systematic approach, grounded in Saaty's relative importance scale and the pairwise comparison of thematic layers, enabled researchers to objectively quantify the relative contributions of each data layer to the delineation of groundwater potential zones (Kumar et al .2016). The allocated ranks and weights for each of the thematic layers taken into account during the analysis are shown in Table 5. The consistency ratio (CR) was determined using the following procedures to assess the consistency of these weight assignments: (1) The eigenvector method was used to obtain the major eigenvalue (λ), as indicated in Table 3, and (2) equation (1) below was used to get the Consistency Index (CI).

$$\boldsymbol{CI} = \frac{\boldsymbol{\lambda_{max} - n}}{\boldsymbol{n-1}} \quad (1)$$

In this case, n stands for the total number of factors used in the analysis. CR=CI/RI is the definition of the consistency ratio, where RI stands for the Random Consistency Index value. Saaty's standard reference provided these RI values (Table 6). Saaty (Saaty & T.L., 1990) states that the analysis can continue if the Consistency Ratio (CR) is 0.10 or less. A CR greater than 0.10 suggests that judgments need to be reevaluated to find and address sources of discrepancy. In pairwise comparisons, a CR score of 0 denotes perfect consistency. The threshold value shows adequate consistency in the judgment matrix, as it is not much greater than 0.1. Equation (2)

was utilized to integrate all ten thematic layers through the weighted overlay analysis approach within a GIS platform to create the groundwater potential zone map of the Rarhu watershed.

$$GWPZ = \sum_{i}^{n}(x_A \times y_B) \quad (2)$$

The weight of the theme layers is represented by X in the equation GWPZ=Groundwater Potential Zone, while the rank of the thematic layers' subclasses is indicated by Y. The thematic map is represented by the term A (A=1, 2, 3,... X), while the thematic map classes are represented by the term B (B=1, 2, 3,.. Y). A larger impact on groundwater potential zones is indicated by a factor with a higher weight value, whereas a smaller impact is suggested by a factor with a lower weight value. Three zones were identified on the final groundwater potential zone map: low, moderate, and high (Arulbalaji et al., 2016). The information about groundwater prospects unique to the Rarhu watershed that was gathered for this study was then used to validate the final product. The flowchart of the approach used in this study is shown in Figure 3.

3. Results and Discussion

3.1.Geology

The geological configuration of an area significantly impacts the presence and distribution of groundwater resources (Yeh et al., 2016). The different geological formations in the research region were identified using the published geological map from the Geological Survey of India (GSI). The Rarhu watershed primarily comprises the Chhota Nagpur Gneissic Complex, encompassing 97.99% of the area, with minor occurrences of the Manbhum Granite (1.54%) and unclassified metamorphic rocks (0.47%) (Fig. 4). The predominant geological units in the study area consist of the Chhota Nagpur gneissic rocks and associated basic rocks (Kumar et al., 2020). During the weighted overlay analysis, a higher weight was assigned to the unclassified metamorphic rocks due to their potential for groundwater occurrence and storage. Conversely, a lower weight was allocated to the Chhota Nagpur Gneissic Complex, reflecting its comparatively lower groundwater prospectivity compared to the metamorphic units. By integrating geological data and assigning appropriate weights based on the hydrogeological characteristics of the rock formations, the researchers aimed to accurately depict the influence of geology on groundwater potential within the Rarhu watershed.

3.2.Geomorphology

Geomorphology, which is a representation of the topography and landform of a region, is one of the main variables that is widely used to define groundwater potential zones. It sheds light on the distribution of different landform characteristics and processes, including freezing and thawing, water flow, geochemical reactions, and temperature variations (Kumar et al., 2016; Rajaveni et al., 2017; Thapa et al., 2017). The study area exhibits a predominantly highland topographic character, characterized by mountainous and undulating terrain features. Approximately 98% of the region is comprised of flood plains and moderately dissected hills, with flood plains

occupying 47% and dissected hills constituting 51.25% of the total area. The western and southwestern sectors of the study area are primarily dominated by hilly terrain. The Pediment Pediplain complex, somewhat divided hills and valleys, water rivers, floodplains, and other bodies of water are among the main geomorphic features. The upstream side of the watershed is predominantly characterized by moderately dissected hills and valleys, featuring sharp but rugged tops indicative of surface runoff affected by erosion. The Pediment Pedi plain complex is prevalent in the midland and lowland areas of the Rarhu watershed. Figure 5 illustrates the geomorphology of the Rarhu watershed, with higher weight assigned to water bodies and lower weight given to lower moderately dissected hills and valleys.

3.3.Land Use and Land Cover (LULC)

Data on land use and land cover (LULC) is essential for understanding infiltration, soil moisture, surface water, groundwater, and groundwater demand. (Yeh et al., 2016; Ibrahim et al., 2016). Many land use classifications, such as deciduous broadleaf forest, agriculture, built-up areas, mixed forest, shrubland, barren land, fallow ground, and water bodies, are noted within the Rarhu watershed (Fig.6). The land use/land cover (LULC) classification analysis reveals that agricultural lands constitute the predominant land cover type, occupying 48% of the study area. Forested areas represent the second most extensive land cover class, covering 24.21% of the region's total extent. Among these, cropland dominates over other categories. The high and midland regions primarily consist of deciduous broadleaf forest, mixed forest, and shrubland, while the lowlands are characterized by built-up areas, water bodies, barren land, shrubland, and fallow land. LULC classes such as forest and cropland significantly contribute to water retention

compared to built-up areas, barren land, and fallow land (Rajaveni et al., 2017). Consequently, higher weight is assigned to deciduous forests, mixed forests, cropland, and water bodies, while lower weight is attributed to built-up areas, shrubland, barren land, and fallow land.

3.4.Lineament Density

Geological structures govern the linear or curved characteristics known as lineaments. They represent areas where there is faulting and fracture, which increases secondary porosity and permeability (Yeh et al., 2016). Lineaments for the study area were acquired from the Bhukosh portal. Subsequently, a lineament density map was generated using GIS software, as shown in (Fig. 7). The results were then carefully examined and divided into five groups: Very Low (0–1,776.42 km/km^2), Low (1,776.43–3,667.45 km/km^2), Moderate (3,667.46–5,959.61 km/km^2), High (5,959.62–8,824.80 km/km^2), and Very High (8,824.81–14,612.5 km/km^2).Lineament density was ranked according to how close together the lineaments were. It has been shown that the strength of groundwater potential reduces with increasing separation from lineaments. Courses with a higher density are given more weight, whereas courses with a lower density are given less weight.

3.5.Drainage Density

Drainage density plays a critical role in groundwater availability and contamination (Ganapuram et al., 2009). It is an inverse function of permeability and a key parameter in delineating groundwater potential zones. The calculation of drainage density involves dividing the aggregate length of all streams within a drainage basin by the drainage basin's entire area (Yeh et al., 2016). Reduced infiltration is

indicated by high drainage densities, which negatively affects an area's capacity for groundwater. On the other hand, low drainage density indicates high infiltration, which increases the possibility of groundwater. Reclassified, the drainage density was divided into five groups: Moderate (2.18–2.72 km/km^2), High (2.73–3.40 km/km^2), Very Low (0–1.53 km/km^2), Low (1.54–2.17 km/km^2), and Very High (3.41–5.26 km/km^2). Low density is given a higher weight in groundwater potential zonation, whereas high density is given a lesser weight. The drainage density map of the Rarhu watershed is seen in Figure 8.

3.6.Slope

One important aspect of the landscape that shows how steep the ground surface is is its slope. It offers crucial details regarding the regionally oriented geological and geodynamic processes (Riley & S.J., 1999). The surface's slope has a big impact on surface runoff and infiltration rates (Singh et al., 2013). Less recharge occurs at higher slope angles because precipitation quickly cascades down steep hills during a downpour. The Rarhu watershed's slope map is shown in Figure 9. The slope values were reclassified and divided into five groups: steep (14.65–23.79), medium (8.38–14.64), mild (4.19–8.37), level (0–4.18), and extremely steep (23.80–66.67). Slopes that are level and mild are given a higher weight, whilst steep and extremely steep slopes are given a lower weight.

3.7. Soil

Soil classes are pivotal in determining the volume of water that can infiltrate into subsurface formations, thereby influencing groundwater recharge (Ibrahim et al., 2016; Das, 2017). When evaluating infiltration rates, soil texture and hydraulic properties are important considerations. The soil map of the Rarhu watershed, shown in Figure 10, shows the several soil groups sandy clay loam

and, loam that were determined using the (FAO) soils. Sandy clay loam soils demonstrate superior infiltration rates in contrast to loam soils, a trait pivotal in influencing infiltration dynamics. This elevated infiltration capacity observed in sandy soils, relative to loam soils, can be attributed to their distinctive textural and structural attributes. Consequently, within the framework of groundwater potential mapping, greater emphasis was placed on the sandy clay loam soil classification to accommodate its heightened efficacy in facilitating infiltration and consequent groundwater replenishment (Essien et al., 2011).

3.8. Rainfall

Rainfall is the main supply of water for the hydrological cycle and has the greatest impact on the dynamics of groundwater in a given area. The study included rainfall data spanning from 1992 to 2022, with an annual rainfall range of 1040mm to 1369mm.Using spatial analysis tools and the Raster calculator, a rainfall spatial distribution map was produced. Based on average values, rainfall was categorized into five groups: Very Low (1040.46–1089.48 mm), Low (1089.49–1151.4 mm), Moderate (1151.41–1215.9 mm), High (1215.91–1293.3 mm), and Very High (1293.31–1363.41 mm). Infiltration is contingent upon rainfall intensity and duration. High-intensity, short-duration rainfall tends to result in less infiltration and more surface runoff, whereas low-intensity, long-duration rainfall encourages higher infiltration than runoff (Ibrahim et al., 2016). Areas with heavy rainfall receive higher weights, and vice versa. The rainfall spatial interpolation map for the Rarhu watershed is shown in Figure 11.

3.9. Topographic Wetness Index (TWI)

The Topographic Wetness Index (TWI), which measures the possible groundwater infiltration driven on by topographical factors, is widely used to evaluate the influence of topography on hydrological processes (Mokarram et al., 2015). TWI calculation employed the "Hydrology tool," a model simulating hydrologic water fluxes throughout the watershed. TWI values in the study area ranged from 1.67 to 20.32. These values were categorized into five groups: 1.67–5.04, 5.05–6.72, 6.73–9.06, 9.07–12.35, and 12.36–20.32. Higher weights were assigned to areas with higher TWI values, and lower weights to those with lower TWI values. Figure 12 shows the Topographic Wetness Index (TWI) map for the Rarhu watershed. The following equation (3) was used to calculate the TWI values:

$$TWI = \ln \frac{\alpha}{\tan \beta} \quad (3)$$

β=Slope-related topographic gradient; α=upslope contributing area.

3.10. Curvature

Concave upward or convex upward profiles are examples of surface profiles whose curvature can be used to quantitatively indicate their nature (Nair et al., 2017). In convex and concave profiles, water tends to accumulate and decelerate, respectively. Within the research area, the curvature ranges varied from 21.76 to -30.72. Five classes (-30.72 to -2.11, -2.10 to -0.67, -0.66 to 0.56, 0.57 to 2.41, and 2.42 to 21.76) were created from the reclassification of these values (Fig. 13). those with greater curvature values were given more weight, whereas those with lower curvature values were given less weight. The Rarhu watershed's curvature map is shown in Figure 13.

3.11. Groundwater Potential Zone (GWPZ)

Throughout the last five to six decades, several anthropogenic activities and imbalanced development have significantly reduced the recharge of groundwater, a replenishable resource. Comprehending the potential of groundwater is essential for the sustainable development and planning of a region. Because groundwater availability fluctuates across time and space, precise and thorough evaluations of groundwater resources are required. Parameters Including Geomorphology, Geology, Land Use/Land Cover (LULC), Lineament, drainage density, Slope, Soil, Rainfall, Curvature, and, Topographic Wetness Index (TWI) are considered in this study. The weighted overlay method was employed to delineate groundwater potential zones of the Rarhu Watershed. The resulting map categorizes areas into high, moderate, and low groundwater potential zones, covering an aerial spread of 50.60 km^2, 329.25 km^2, and 220.68 km^2 respectively (Table 7). Midland and lowland regions are home to the majority of high groundwater potential zones, which are often found in places with significant rainfall and high infiltration potential. Valleys and places with high drainage densities are typical locations for zones with moderate groundwater potential. Low groundwater potential zones are less common in midland regions and more common in highlands and lowlands (Fig. 14). The Gneiss complex, steep slopes, high drainage density, and conserved forests are all linked to these low potential zones. To further validate the delineated groundwater potential zones, the results obtained in this study were compared against observation well data from the Central Ground Water Board (CGWB). For this purpose, a comprehensive analysis was conducted on a total of 32 observation wells located within the study area. The groundwater levels and yields recorded at these observation wells were cross-referenced with the mapped groundwater potential zones, providing an additional layer of verification for the study's findings.

3.12. Validation of GPZ

The range of values for the area under the curve (AUC) is 0.5 to 1.0. According to Rasyid et al., (2016), the AUC can be divided into five classes for improved predictive performance evaluation: 0.5–0.6 (unacceptable discrimination), 0.6–0.7 (bad discrimination), 0.7–0.8 (acceptable discrimination), 0.8–0.9 (good discrimination), and 0.9–1.0 (outstanding discrimination). The greater discriminating and prediction power of the model is shown by higher AUC values. To validate the delineated groundwater potential zones, a comprehensive dataset was compiled, consisting of 32 observation wells (including borewells, tube wells, and dug wells) and 16 non-well point locations. The spatial coordinates were gathered during field surveys in May 2023 using Garmin Etrix 30x GPS receivers. Borewell and dug well locations from the Central Ground Water Board (CGWB, 2022), Ranchi Jharkhand supplemented the field data. This dataset served as a reference for evaluating the accuracy and reliability of the groundwater potential zone mapping. The AUC analysis yielded a value of 0.877, indicating a considerably acceptable accuracy for the predicted groundwater potential zones (GPZs) model (Fig. 8). ROC curve analysis confirmed the effective prediction of GPZs using the Analytical Hierarchy Process (AHP) methodology, with an AUC value of 0.877. According to Rasyid et al., (2016), an AUC value within the 0.8–0.9 range signifies very good acceptable model discrimination and predictive performance (Fig. 15). Thus, the obtained AUC value validates the robustness of the AHP-based approach for delineating groundwater potential zones in the study area.

3.13. Limitations of the study

The geological complexity of the study areas poses a significant challenge for this research. Determining groundwater potential zones is complicated by the heterogeneity resulting from various rock types, geological formations, and structural features like folds and faults. Additionally, uncertainties related to hydrogeological factors, particularly hydraulic conductivity, can greatly affect the precision of zone definitions. The lack of thorough understanding of these hydrogeological characteristics inherently obscures the results of groundwater potential mapping efforts. Integrating advanced modeling tools and high-resolution data is essential for future research endeavors to enhance the reliability of groundwater potential assessments in light of these geological and hydrogeological complexities.

4. Conclusions

The current study aims to map groundwater potential zones in the Rarhu River watershed, a small dry tropical region in east India, by employing a blend of AHP and GIS techniques. This watershed lies on the eastern side of the Ranchi plateau and the western side of the Purulia hills. The final groundwater potential zone map facilitated the categorization of the study area into three distinct classes: high, moderate, and, low potential zones. The spatial distribution of these zones revealed that the high-potential zones are predominantly situated in the lower catchment and middle reaches of the river. In contrast, the low and moderate potential zones are primarily located within the medium to high altitudes and, migmatite complex formation region of the watershed. The moderate potential zone exhibits a widespread distribution, encompassing 53.83% of the total study area. The high and low potential zones cover 8.43 % and 36.75 % of the area, respectively. This spatial distribution pattern of groundwater potential zones is influenced by

the interplay of various hydrogeological factors, including geological formations, geomorphological features, and hydrological characteristics of the watershed. The groundwater potential zone map provides insights for decision-makers on groundwater planning and management for urban and agricultural purposes. As most of the study area is agricultural land, the findings can help improve irrigation facilities and enhance agricultural productivity. By identifying areas with varying groundwater prospectivity, the map supports sustainable groundwater utilization strategies tailored to the region's hydrogeological conditions and water demands. It serves as a valuable decision-support tool for stakeholders to develop informed strategies for judicious groundwater management.

CRediT authorship contribution statement

Rupa Sharma: Data preparation, Writing – review & editing, and analysis. Rahul Kumar Pandey:Conceptualization, Methodology, Writing – original draft, Writing – review & editing. Abhay Krishna Singh: Formal analysis, review &editings. All the authors have read, reviewed, and approved the submitted manuscript.

References

Adiat, K. A. N., Nawawi, M. N. M., & Abdullah, K. (2012). Assessing the accuracy of GIS-based elementary multi criteria decision analysis as a spatial prediction tool–a case of predicting potential zones of sustainable groundwater resources. Journal of Hydrology, 440, 75-89.

Agarwal, E., Agarwal, R., Garg, R. D., & Garg, P. K. (2013). Delineation of groundwater potential zone: An AHP/ANP approach. Journal of earth system science, 122, 887-898.

Arulbalaji, P., &Gurugnanam, B. (2016). An integrated study to assess the groundwater potential zone using geospatial tool in Salem District, South India. J HydrogeolHydrol Eng. of, 7, 2.

Arulbalaji, P., Padmalal, D., &Sreelash, K. (2019). GIS and AHP techniques-based delineation of groundwater potential zones: a case study from southern Western Ghats, India. Scientific reports, 9(1), 2082.

Arulbalaji, P., Padmalal, D., &Sreelash, K. (2019). GIS and AHP techniques based delineation of groundwater potential zones: a case study from southern Western Ghats, India. Scientific reports, 9(1), 2082.

Asoka, A., Wada, Y., Fishman, R., & Mishra, V. (2018). Strong linkage between precipitation intensity and monsoon season groundwater recharge in India. Geophysical Research Letters, 45(11), 5536-5544.

Banerjee, K., Santhosh Kumar, M. B., Tilak, L. N., &Vashistha, S. (2021). Analysis of groundwater quality using GIS-based water quality index in Noida, Gautam Buddh Nagar, Uttar Pradesh (UP), India. In Applications of Artificial Intelligence and Machine Learning: Select Proceedings of ICAAAIML 2020 (pp. 171-187). Springer Singapore.

Bera, A., Mukhopadhyay, B. P., & Barua, S. (2020). Delineation of groundwater potential zones in Karha river basin, Maharashtra, India, using AHP and geospatial techniques. Arabian Journal of Geosciences, 13(15), 693.

Central Ground Water Board (CGWB) (2022). Ministry of Jal Shakti, Department of Water Resourceshttps://cgwb.gov.in/cgwbpnm/public/uploads/documents/16883646811420506028file.pdf

Changnon, S. A., Huff, F. A., & Hsu, C. F. (1988). Relations between precipitation and shallow groundwater in Illinois. Journal of Climate, 1(12), 1239-1250.

Chenini, I. &Mammou, A. Ben. Groundwater recharge study in arid region: an approach using GIS techniques and numerical modeling. Comput. Geosci. 36, 801–817 (2010).

Corsini, A., Cervi, F., & Ronchetti, F. (2009). Weight of evidence and artificial neural networks for potential groundwater spring mapping: an application to the Mt. Modino area (Northern Apennines, Italy). Geomorphology, 111(1-2), 79-87.

Dar, I. A., Sankar, K., & Dar, M. A. (2010). Remote sensing technology and geographic information system modeling: an integrated approach towards the mapping of groundwater potential zones in Hardrock terrain, Mamundiyar basin. Journal of Hydrology, 394(3-4), 285-295.

Dar, I. A., Sankar, K., & Dar, M. A. (2011). Deciphering groundwater potential zones in hard rock terrain using geospatial technology. Environmental monitoring and assessment, 173, 597-610.

Dar, T., Rai, N., & Bhat, A. (2021). Delineation of potential groundwater recharge zones using analytical hierarchy process (AHP). Geology, Ecology, and Landscapes, 5(4), 292-307.

Das, D. (2000). GIS application in hydrogeological studies. GISdevelopment. net. http://www. gisdevelopment. net/application/nrm/water/overview/wato0003pf. htm.

Das, S. (2017). Delineation of groundwater potential zone in hard rock terrain in Gangajalghati block, Bankura district, India using remote sensing and GIS techniques. Modeling Earth Systems and Environment, 3(4), 1589-1599.

Dhawan, V. (2017, January). Water and agriculture in India. In Background paper for the South Asia expert panel during the Global Forum for Food and Agriculture (Vol. 28, pp. 80-85). OAV German Asia-Pacific Business Association.

Essien, O. E. (2011). Effect of varying rates of organic amendments on porosity and infiltration rate of sandy loam soil.

FAUST, N., ANDERSON, W., & STAR, J. (1991). Geographic information systems and remote sensing future computing environment. Photogrammetric Engineering and Remote Sensing, 57(6), 655-668.

Ganapuram, S., Kumar, G. V., Krishna, I. M., Kahya, E., & Demirel, M. C. (2009). Mapping of groundwater potential zones in the Musi basin using remote sensing data and GIS. Advances in Engineering Software, 40(7), 506-518.

Ghosh, P. K., Bandyopadhyay, S., & Jana, N. C. (2016). Mapping of groundwater potential zones in hard rock terrain using geoinformatics: a case of Kumari watershed in western part of West Bengal. Modeling Earth Systems and Environment, 2, 1-12.

Guria, R., Mishra, M., Dutta, S., da Silva, R. M., & Santos, C. A. G. (2024). Remote sensing, GIS, and analytic hierarchy process-based delineation and sustainable management of potential groundwater zones: a case study of Jhargram district, West Bengal, India. Environmental Monitoring and Assessment, 196(1), 1-30.

Hinton, J. C. (1996). GIS and remote sensing integration for environmental applications. International Journal of Geographical Information Systems, 10(7), 877-890.

Ibrahim-Bathis, K., & Ahmed, S. A. (2016). Geospatial technology for delineating groundwater potential zones in Doddahalla watershed of Chitradurga district, India. The Egyptian Journal of Remote Sensing and Space Science, 19(2), 223-234.

Ifediegwu, S. I. (2022). Assessment of groundwater potential zones using GIS and AHP techniques: a case study of the Lafia district, Nasarawa State, Nigeria. Applied Water Science, 12(1), 10.

India: India's Water Economy, Bracing for a Turbulent Future - 2006; Report No. 34750-IN, Agriculture and Rural Development Unit South Asia Region, Document of the World Bank.

Israil, M., Al-Hadithi, M., & Singhal, D. C. (2006). Application of a resistivity survey and geographical information system (GIS) analysis for hydrogeological zoning of a piedmont area, Himalayan foothill region, India. Hydrogeology Journal, 14, 753-759.

Jha, M. K., Chowdhury, A., Chowdary, V. M., & Peiffer, S. (2007). Groundwater management and development by integrated remote sensing and geographic information systems: prospects and constraints. Water resources management, 21, 427-467.

Kom, K. P., Gurugnanam, B., & Sunitha, V. (2024). Delineation of groundwater potential zones using GIS and AHP techniques in Coimbatore district, South India. International Journal of Energy and Water Resources, 8(1), 85-109.

Kumar, D., Mondal, S., & Warsi, T. (2020). Deep insight to the complex aquifer and its characteristics from high resolution electrical resistivity tomography and borehole studies for groundwater exploration and development. Journal of Earth System Science, 129(1), 68.

Kumar, P., Herath, S., Avtar, R., & Takeuchi, K. (2016). Mapping of groundwater potential zones in Killinochi area, Sri Lanka, using GIS and remote sensing techniques. Sustainable Water Resources Management, 2, 419-430.

Lee, S., Kim, Y. S., & Oh, H. J. (2012). Application of a weights-of-evidence method and GIS to regional groundwater productivity potential mapping. Journal of Environmental Management, 96(1), 91-105.

Magesh, N. S., Chandrasekar, N., &Soundranayagam, J. P. (2012). Delineation of groundwater potential zones in Theni district, Tamil Nadu, using remote sensing, GIS and MIF techniques. Geoscience frontiers, 3(2), 189-196.

Mogaji, K. A., Lim, H. S. & Abdullah, K. Regional prediction of groundwater potential mapping in a multifaceted geology terrain using GIS-based Dempster–Shafer model. Arab. J. Geosci. 8, 3235–3258 (2015).

Moghaddam, D. D., Rezaei, M., Pourghasemi, H. R., Pourtaghie, Z. S., & Pradhan, B. (2015). Groundwater spring potential mapping using bivariate statistical model and GIS in the Taleghan watershed, Iran. Arabian Journal of Geosciences, 8, 913-929.

Moharir, K. N., Pande, C. B., Gautam, V. K., Singh, S. K., & Rane, N. L. (2023). Integration of hydrogeological data, GIS and AHP techniques applied to delineate groundwater potential zones in sandstone, limestone and shales rocks of the Damohdistrict,(MP) central India. Environmental research, 228, 115832.

Mokarram, M., Roshan, G., & Negahban, S. (2015). Landform classification using topography position index (case study: salt dome of Korsia-Darab plain, Iran). Modeling Earth Systems and Environment, 1, 1-7.

Mukherjee, S., Mukherjee, S., Garg, R. D., Bhardwaj, A., & Raju, P. L. N. (2013). Evaluation of topographic index in relation to terrain roughness and DEM grid spacing. Journal of Earth System Science, 122, 869-886.

Murmu, P., Kumar, M., Lal, D., Sonker, I., & Singh, S. K. (2019). Delineation of groundwater potential zones using geospatial techniques and analytical hierarchy process in Dumka district, Jharkhand, India. Groundwater for Sustainable Development, 9, 100239.

Naghibi, S. A., Pourghasemi, H. R., Pourtaghi, Z. S. & Rezaei, A. Groundwater qanat potential mapping using frequency ratio and Shannon's entropy models in the Moghan watershed, Iran. Earth Sci. Informatics 8, 171–186 (2015).

Nair, H. C., Padmalal, D., Joseph, A., & Vinod, P. G. (2017). Delineation of groundwater potential zones in river basins using geospatial tools—an example from Southern Western Ghats, Kerala, India. Journal of Geovisualization and Spatial Analysis, 1, 1-16.

Nampak, H., Pradhan, B. & Manap, M. A. Application of GIS based data driven evidential belief function model to predict groundwater potential zonation. J. Hydrol. 513, 283–300 (2014).

National water policy. (2022). https://nwm.gov.in/sites/default/files/nwp20025617515534.pdf

NITI Aayog – Annual Report 2017-2018, Government of India. https://www.niti.gov.in/writereaddata/files/document.../AnnualReport-English.pdf.

Oh, H. J., Kim, Y. S., Choi, J. K., Park, E., & Lee, S. (2011). GIS mapping of regional probabilistic groundwater potential in the area of Pohang City, Korea. Journal of Hydrology, 399(3-4), 158-172.

Ozdemir, A. (2011). GIS-based groundwater spring potential mapping in the Sultan Mountains (Konya, Turkey) using frequency ratio, weights of evidence and logistic regression methods and their comparison. Journal of hydrology, 411(3-4), 290-308.

Panahi, M. R., Mousavi, S. M., &Rahimzadegan, M. (2017). Delineation of groundwater potential zones using remote sensing, GIS, and AHP technique in Tehran–Karaj plain, Iran. Environmental earth sciences, 76, 1-15.

Pourghasemi, H. R. &Beheshtirad, M. Assessment of a data-driven evidential belief function model and GIS for groundwater potential mapping in the Koohrang Watershed, Iran. Geocarto Int. 30, 662–685 (2015).

Pourtaghi, Z. S., & Pourghasemi, H. R. (2014). GIS-based groundwater spring potential assessment and mapping in the Birjand Township, southern Khorasan Province, Iran. Hydrogeol J, 22(3), 643-662.

Pradhan, B. (2009). Groundwater potential zonation for basaltic watersheds using satellite remote sensing data and GIS techniques. Central European Journal of Geosciences, 1, 120-129.

Rahmati, O., Nazari Samani, A., Mahdavi, M., Pourghasemi, H. R., &Zeinivand, H. (2015). Groundwater potential mapping at Kurdistan region of Iran using analytic hierarchy process and GIS. Arabian Journal of Geosciences, 8, 7059-7071.

Rahmati, O., Pourghasemi, H. R., & Melesse, A. M. (2016). Application of GIS-based data driven random forest and maximum entropy models for groundwater potential mapping: a case study at Mehran Region, Iran. Catena, 137, 360-372.

Rajasekhar, M., Upendra, B., Raju, G. S., & Anand. (2022). Identification of groundwater potential zones in southern India using geospatial and decision-making approaches. Applied Water Science, 12(4), 68.

Rajaveni, S. P., Brindha, K., & Elango, L. (2017). Geological and geomorphological controls on groundwater occurrence in a hard rock region. Applied water science, 7, 1377-1389.

Rasyid, A. R., Bhandary, N. P., & Yatabe, R. (2016). Performance of frequency ratio and logistic regression model in creating GIS based landslides susceptibility map at Lompobattang Mountain, Indonesia. Geoenvironmental Disasters, 3, 1-16.

Razandi, Y., Pourghasemi, H. R., Neisani, N. S., & Rahmati, O. (2015). Application of analytical hierarchy process, frequency ratio, and certainty factor models for groundwater potential mapping using GIS. Earth Science Informatics, 8, 867-883.

Riley, S. J., DeGloria, S. D., & Elliot, R. (1999). Index that quantifies topographic heterogeneity. intermountain Journal of sciences, 5(1-4), 23-27.

Russo, T. A., Fisher, A. T., & Lockwood, B. S. (2015). Assessment of managed aquifer recharge site suitability using a GIS and modeling. Groundwater, 53(3), 389-400.

Saaty, T. L. (1990). Decision making for leaders: the analytic hierarchy process for decisions in a complex world. RWS publications.

Singh, A., Kumar, R., Kumar, R., Pippal, P. S., Sharma, P., & Sharma, A. (2024). Delineation of Groundwater Potential zone using geospatial tools and Analytical Hierarchy Process (AHP) in the State of Uttarakhand, India. Advances in Space Research, 73(6), 2939-

S. N	Study Area	G	GM	LULC	LD	DD	SL	S	RF	TWI	CUR	E	TRI	Literature

2954.

Singh, P., Thakur, J. K., & Kumar, S. (2013). Delineating groundwater potential zones in a hard-rock terrain using geospatial tool. Hydrological Sciences Journal, 58(1), 213-223.

Thapa, R., Gupta, S., & Reddy, D. V. (2017). Application of geospatial modelling technique in delineation of fluoride contamination zones within Dwarka Basin, Birbhum, India. Geoscience Frontiers, 8(5), 1105-1114.

World Bank. (2005). India's water economy: Bracing for a turbulent future. Report No. 34750-IN.

Yeh, H. F., Cheng, Y. S., Lin, H. I., & Lee, C. H. (2016). Mapping groundwater recharge potential zone using a GIS approach in Hualian River, Taiwan. Sustainable Environment Research, 26(1), 33-43.

1	Uttarakhand, India	√	√	√	-	√	√	√	√	√	√	-	-	Singh et al., 2024
2	Jhargram, West Bengal	√	√	√	√	√	√	√	√	√	√	√	√	Guria et al., 2024
3	Domah (M.P)	-	√	√	√	√	√	√	-	√	-	-	√	Moharir et al., 2023
4	Coimbatore, South India	√	√	√	√	√	√	√	√	√	√	-	-	Kom et al., 2022
5	Anantapur (A.P)	√	√	√	√	√	√	√	√	-	-	-	-	Rajasekhar et al., 2022
6	Nasarawa State, Nigeria	√	√	√	√	√	√	√	√	-	-	-	-	Ifediegwu 2022
7	Kashmir valley	-	√	√	√	√	√	√	√	-	-	-	-	Dar et al., 2021
8	Gautham Buddh Nagar (U.P)	√	√	√	-	√	√	√	-	-	-	-	-	Banerjee et al., 2021
9	Karha (Maharashtra)	√	√	√	√	√	√	√	√	√	√	-	-	Bera et al., 2020
10	Southern Western Ghats	√	√	√	√	√	√	√	√	√	√	-	-	Arulbalaji et al., 2019
11	Dumka (Jharkhand)	-	√	√	√	√	√	√	√	-	-	-	-	Murmu et al., 2019
12	Tehran (Iran)	√	-	√	√	√	√	√	√	-	-	-	-	Panahi et al., 2017
13	Unnao (U.P)	√	√	√	√	√	√	√	√	-	-	-	-	Agarwal et al., 2013
Current Study	Rarhu watershed, Jharkhand	√	√	√	√	√	√	√	√	√	√	-	-	

Table 1: A literature overview of various parameters employed in global and regional studies for delineating groundwater potential zones utilizing the Analytical Hierarchy Process (AHP) method.

Table 2: This section elucidates the diverse datasets utilized in the study, detailing their respective sources and applications in generating thematic layers for the delineation of groundwater potential zones.

Types of Data	Scale/Resolution	Parameter	Sources Data
ALOS DEM	12.5 m	Slope, Elevation, and, curvature	Earth Data (https://search.asf.alaska.edu/)
Topographical maps	1: 50000 RF	Drainage density and, lineament density map	Onlinemaps Portal (https://onlinemaps.surveyofindia.gov.in/)
Geological and Geomorphological	2M	Geology and Geomorphology map	Bhukosh (https://bhukosh.gsi.gov.in)
Rainfall data	0.25*0.25 degree	30 years average (1992 - 2022)	IMD (https://www.imdpune.gov.in)
Soil data	1: 1250000	Soil texture map	FAO Soils Portal (https://www.fao.org/soils-portal)
Sentinel 2A	10 m	LULC	ESRI Land Cover (https://livingatlas.arcgis.com/landcover/)
Groundwater	Well depth	Method Validation	CGWB 2022 (https://cgwb.gov.in/cgwbpnm/public/uploads/documents/16883646811420506028file.pdf)

Table 3: Pairwise comparison matrix incorporating the relative importance weights assigned to the ten thematic layers employed in the present study.

Parameters	RF	LULC	GM	G	S	DD	SL	LD	CUR	TWI
RF	1	1/3	1	1/5	1	1	1/3	1	1/3	1/3
LULC	3	1	3	1/3	1	1	1	1	1/3	1
GM	1	1/3	1	1/3	1	1	1/3	1	1/5	1/3
G	5	3	3	1	1	3	3	1	1	3
S	1	1	1	1	1	3	1	1	1/5	1
DD	1	1	1	1/3	1/3	1	1	5	1	1
SL	3	1	3	1/3	1	1	1	1	1/3	1
LD	1	1	1	1	1	1/5	1	1	1/3	1
CUR	3	3	5	1	5	1	3	3	1	3
TWI	3	1	3	1/3	1	1	1	1	1/3	1
Sum	22.00	12.67	22.00	5.87	13.33	13.20	12.67	16.00	5.07	12.67

Table 4: Normalized pairwise comparison matrix and the corresponding weights assigned to each parameter influencing the distribution of groundwater potential in the present study.

Parameters	RF	LULC	GM	G	S	DD	SL	LD	CUR	TWI	Lamda max	CI	CR	NPE
RF	1.00										11.135	1.49	0.085	0.160
LULC	0.33	1.00												0.086
GM	0.20	0.33	1.00											0.047
G	0.33	1.00	3.00	1.00										0.086
S	1.00	1.00	1.00	1.00	1.00									0.097
DD	1.00	3.00	3.00	3.00	1.00	1.00								0.158
SL	1.00	1.00	1.00	1.00	1.00	1.00	1.00							0.135
LD	1.00	1.00	3.00	1.00	3.00	1.00	0.20	1.00						0.106
CUR	0.33	0.33	1.00	0.33	0.20	0.20	0.33	1.00	1.00					0.038
TWI	0.33	1.00	3.00	1.00	1.00	0.33	1.00	1.00	3.00	1.00				0.086

Table 5: Categorization of key factors influencing the spatial distribution of Groundwater Potential Zones in the present study.

Parameters	Parameters class	Area (km²)	Area(%)	Rating	AHP weight
Rainfall	1040.46 – 1089.48	57.15	9.52	1	0.160
	1089.49 – 1151.4	185.83	30.94	2	
	1151.41 – 1215.9	90.56	15.08	3	
	1215.91 – 1293.3	171.26	28.52	4	
	1293.31 – 1363.41	95.73	15.94	5	
LULC	Deciduous broadleaf	145.38	24.21	3	0.086
	Crop land	288.55	48.05	2	
	Built up	5.56	0.93	1	
	Mixed forest	59.99	9.99	3	
	Shrub land	65.40	10.89	2	
	Barren land	9.85	1.64	2	
	Fallow land	15.76	2.62	3	
	Water bodies	10.05	1.67	5	
Geomorphology	Flood plain	282.27	47.0	4	0.047
	Moderately dissected hills	3.7.75	51.25	2	
	Pediment pediplain complex	1.18	0.20	3	
	Waterbodies other	8.69	1.45	5	
	Waterbody river	0.64	0.11	5	
Geology	Unclassified metamorphic	2.85	0.47	5	0.086
	Manbhum Granite	9.22	1.54	1	
	Chhotanagpur Gneissic complex	588.46	97.99	3	
Soil	Sandy clayloam	398.99	66.44	5	0.097
	Loam	201.54	33.56	3	
Drainage density	0 -1.53	51.45	8.57	1	0.158
	1.54 – 2.17	143.40	23.88	2	
	2.18 – 2.72	202.36	33.70	3	
	2.73 – 3.4	160.76	26.77	4	
	3.41 – 5.26	42.57	7.09	5	
Slope	0 – 4.18	279	46.46	5	0.135
	4.19 – 8.37	197.20	32.84	4	
	8.38 – 14.64	77.61	12.92	3	
	14.65 – 23.79	33.37	5.56	2	
	23.8 – 66.67	13.35	2.22	1	
Lineament density	0 – 1,776.42	202.36	33.70	5	0.106
	1776.43-3,667.45	172.32	28.69	4	
	3667.46-5,959.61	119.17	19.84	3	
	5,959.62-8,824.8	73.36	12.22	2	
	8,824.81-14612.5	33.33	5.55	1	
Curvature	-30.72- 2.11	23.69	3.95	1	0.038
	-2.1 - -0.67	194.75	32.43	2	
	-0.66- 0.56	275.76	45.92	3	
	0.57 – 2.41	102.94	17.14	4	
	2.42 – 21.76	3.39	0.56	5	
TWI	1.67 – 5.04	211	35.14	5	0.086
	5.05 – 6.72	267.22	44.50	4	
	6.73 – 9.06	84.69	14.10	3	
	9.07 – 12.35	29.51	4.91	2	
	12.36 – 20.32	8.11	1.35	1	

Table 6: The random consistency index (RI) values corresponding to different matrix orders (n), as established by Saaty (1990).

No	1	2	3	4	5	6	7	8	9	10
RI	0.00	0.00	0.58	0.89	1.12	1.25	1.32	1.40	1.45	1.49

Table 7: The extent of groundwater potential zones identified in the study area.

GWPZ Class	Area (Km2)	Area %	Potential Capacity
Low	220.68	36.75	Poor
Moderate	329.25	54.83	Moderate
High	50.60	8.43	Good
Total	600.53	100	

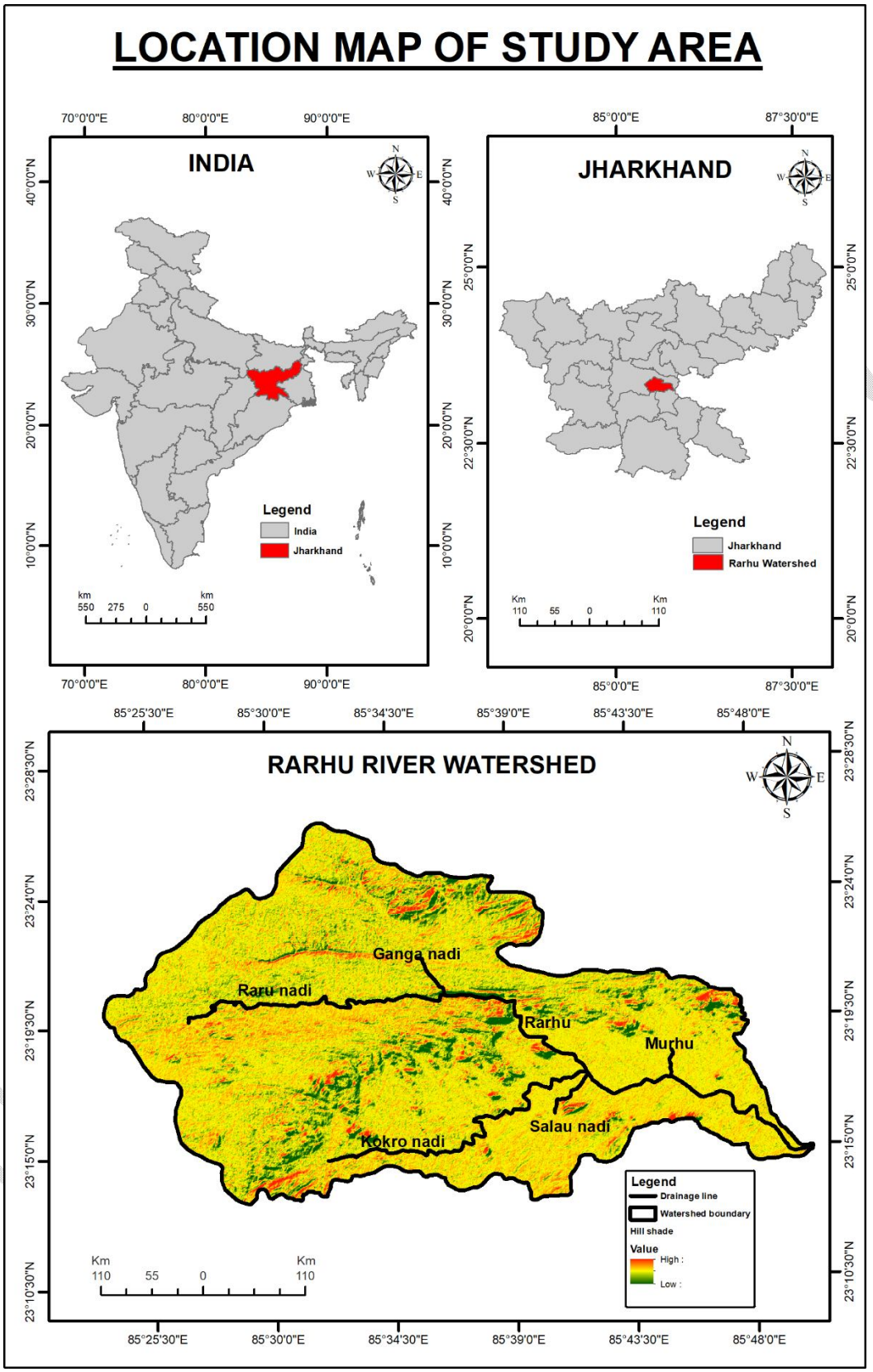

Fig 1.Showing the location map of the study area.

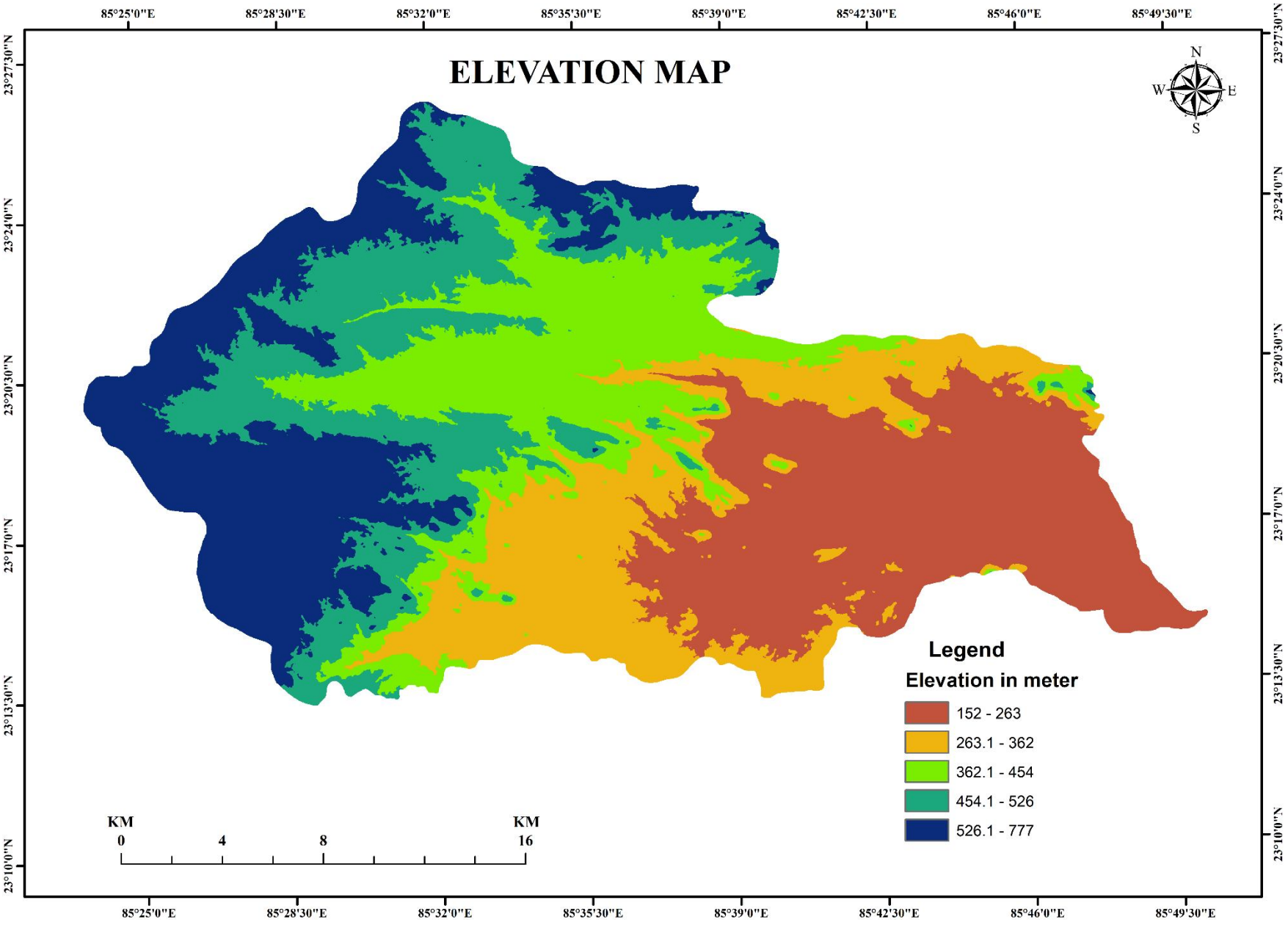
ELEVATION MAP
85°25'0"E
85°28'30"E
85°32'0"E
85°35'30"E
85°39'0"E
85°42'30"E
85°46'0"E
85°49'30"E
23°27'30"N
23°24'0"N
23°20'30"N
23°17'0"N
23°13'30"N
23°10'0"N
N
W
E
S
Legend
Elevation in meter
152 - 263
263.1 - 362
362.1 - 454
454.1 - 526
526.1 - 777
KM
0
4
8
16

Fig 2. Showing the Elevation map of the study area.

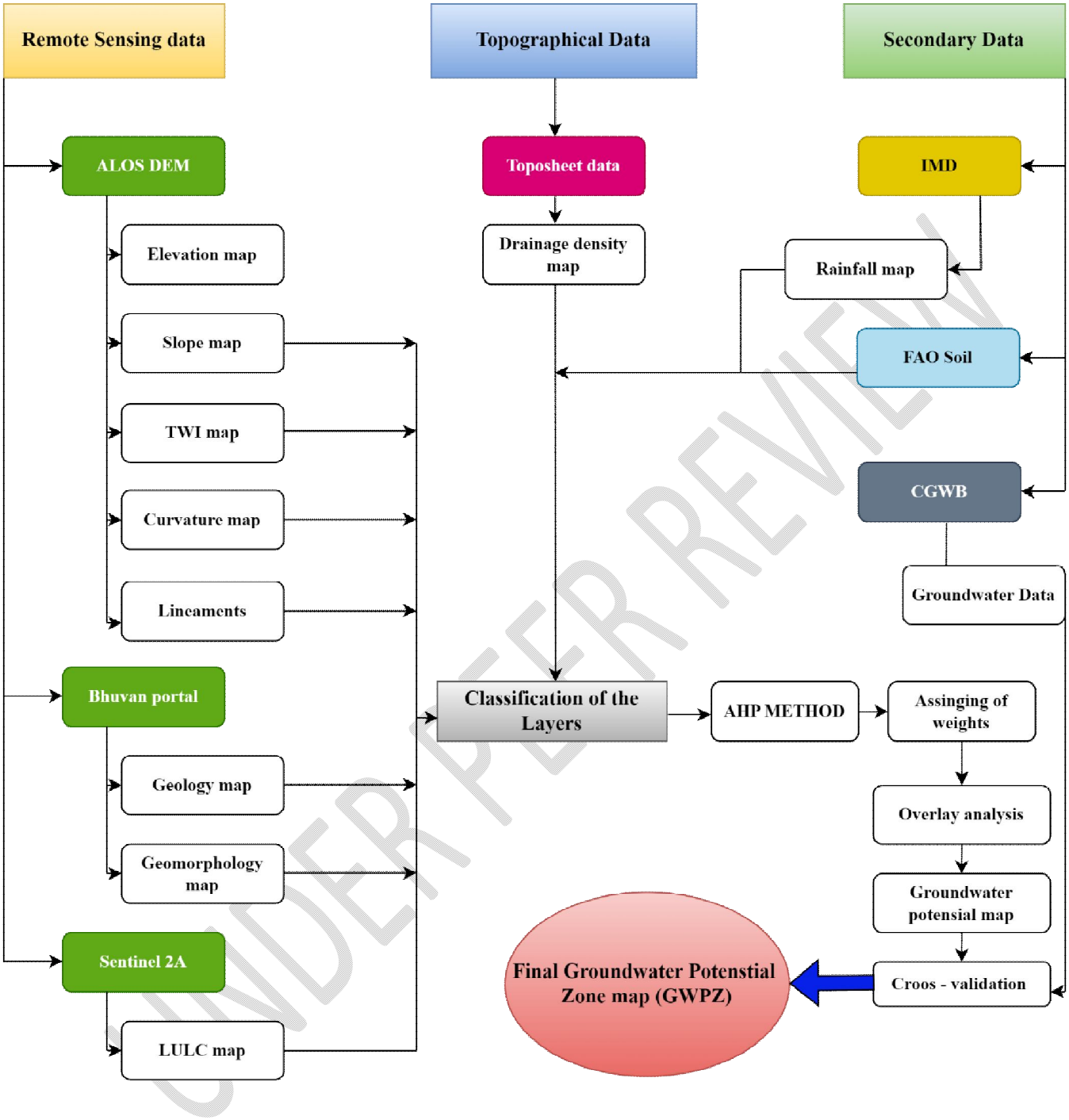

Fig 3. Schematic flowchart illustrating the methodological framework employed for the delineation and mapping of Groundwater Potential Zones.

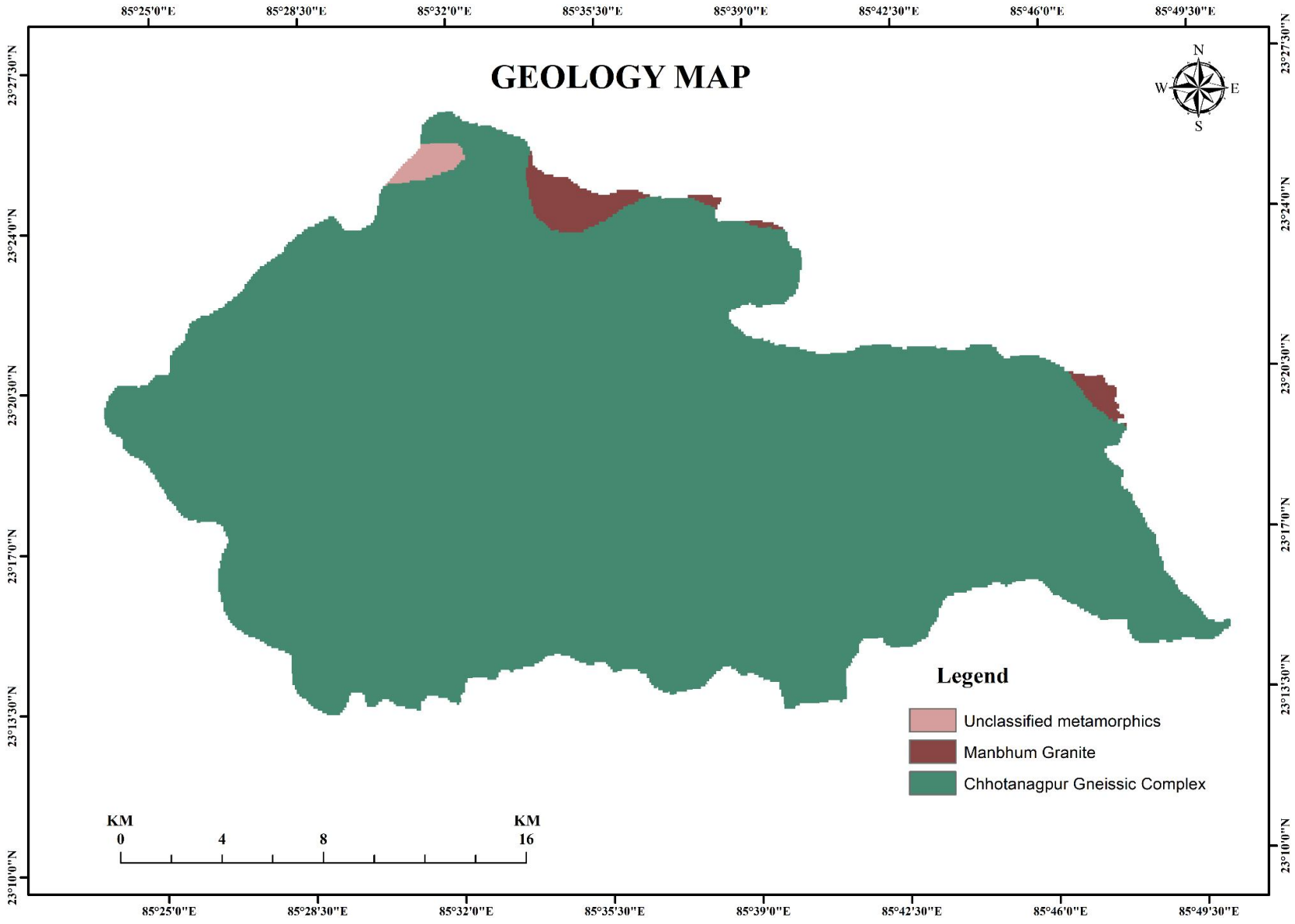
GEOLOGY MAP
85°25'0"E
85°28'30"E
85°32'0"E
85°35'30"E
85°39'0"E
85°42'30"E
85°46'0"E
85°49'30"E
23°27'30"N
23°24'0"N
23°20'30"N
23°17'0"N
23°13'30"N
23°10'0"N
N
W
E
S
Legend
Unclassified metamorphics
Manbhum Granite
Chhotanagpur Gneissic Complex
KM
0
4
8
KM
16

Fig 4.Showing the Geology map of the study area.

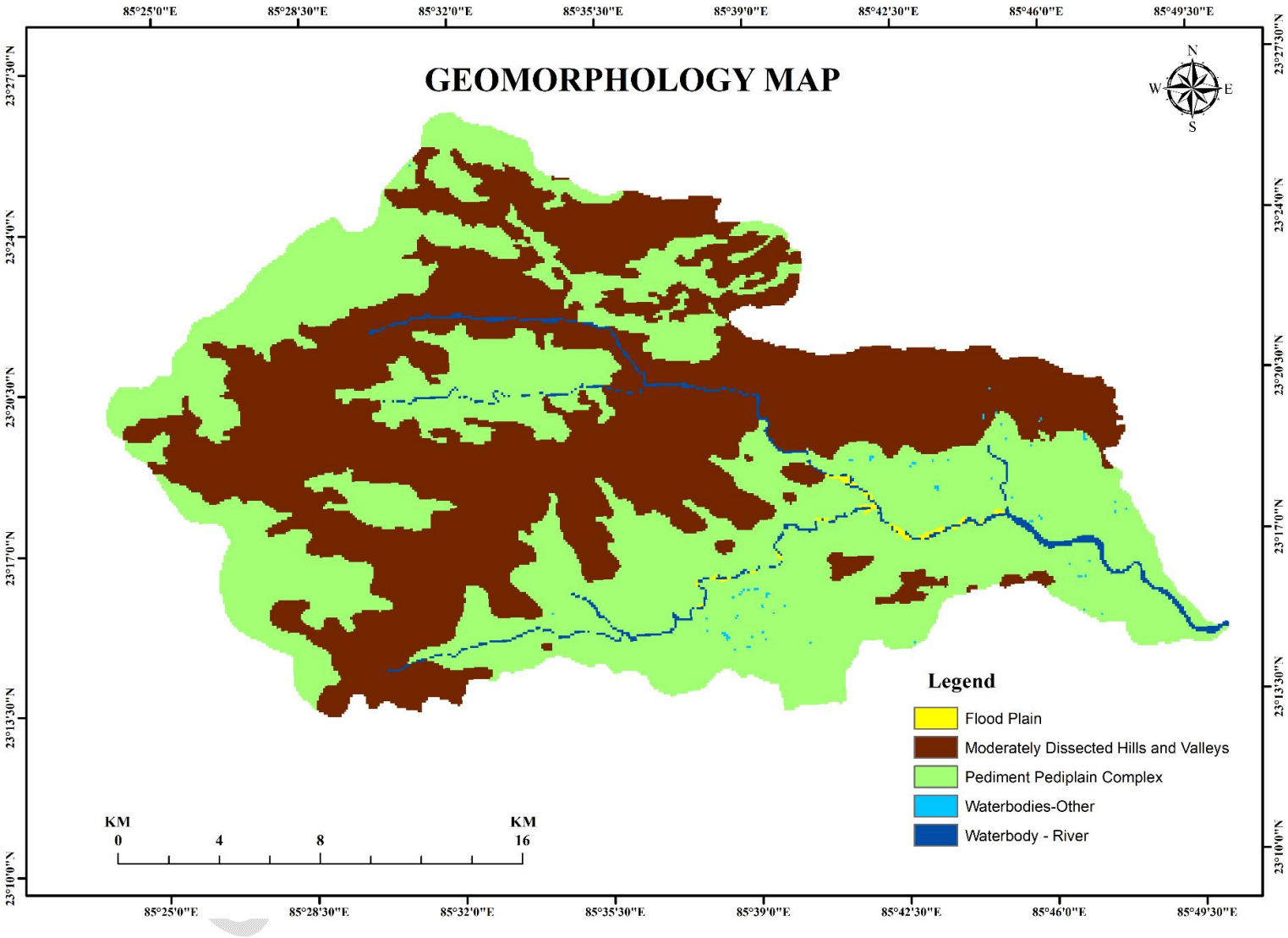
GEOMORPHOLOGY MAP
N
W
E
S
85°25'0"E
85°28'30"E
85°32'0"E
85°35'30"E
85°39'0"E
85°42'30"E
85°46'0"E
85°49'30"E
23°27'30"N
23°24'0"N
23°20'30"N
23°17'0"N
23°13'30"N
23°10'0"N
Legend
Flood Plain
Moderately Dissected Hills and Valleys
Pediment Pediplain Complex
Waterbodies-Other
Waterbody - River
KM
0
4
8
16

Fig 5.Showing the Geomorphology map of the study area.

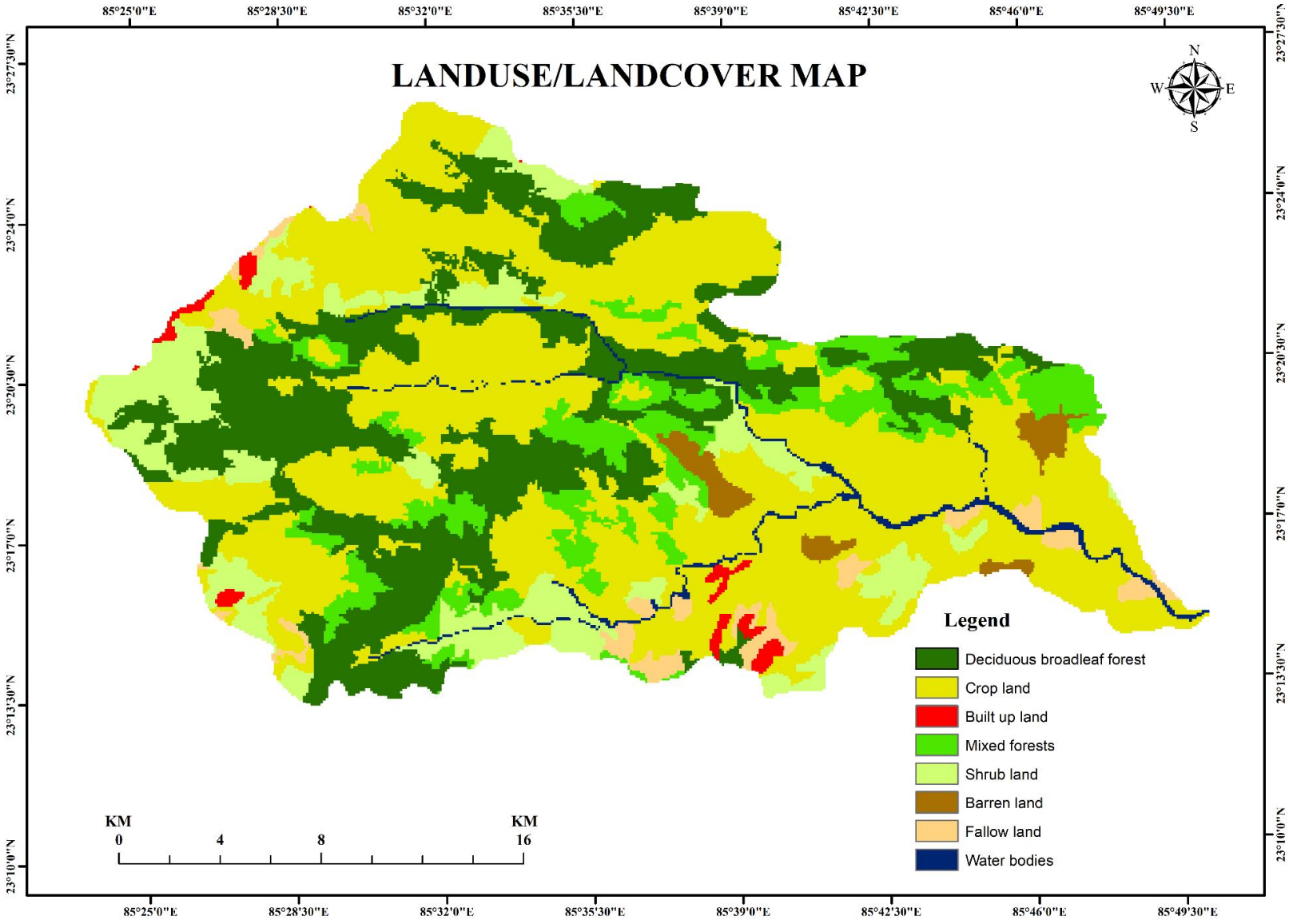
LANDUSE/LANDCOVER MAP
N
W
E
S
85°25'0"E
85°28'30"E
85°32'0"E
85°35'30"E
85°39'0"E
85°42'30"E
85°46'0"E
85°49'30"E
23°27'30"N
23°24'0"N
23°20'30"N
23°17'0"N
23°13'30"N
23°10'0"N
Legend
Deciduous broadleaf forest
Crop land
Built up land
Mixed forests
Shrub land
Barren land
Fallow land
Water bodies
KM
0
4
8
KM
16

Fig 6. Showing the Land use and land cover (LULC) map of the study area.

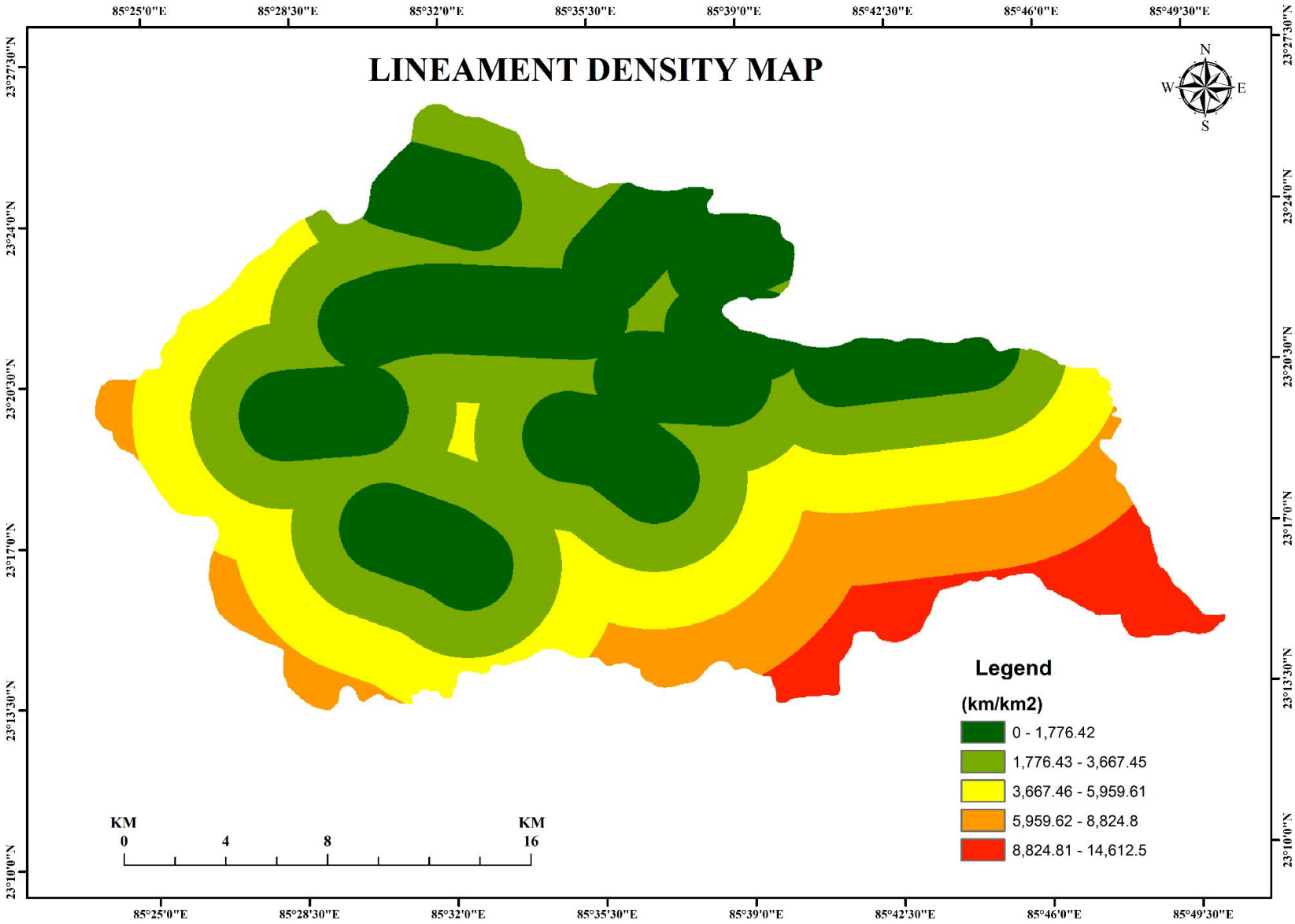
LINEAMENT DENSITY MAP
85°25'0"E
85°28'30"E
85°32'0"E
85°35'30"E
85°39'0"E
85°42'30"E
85°46'0"E
85°49'30"E
23°27'30"N
23°24'0"N
23°20'30"N
23°17'0"N
23°13'30"N
23°10'0"N
N
W
E
S
Legend
(km/km2)
0 - 1,776.42
1,776.43 - 3,667.45
3,667.46 - 5,959.61
5,959.62 - 8,824.8
8,824.81 - 14,612.5
KM
0
4
8
KM
16

Fig 7. Showing the Lineament density map of the study area.

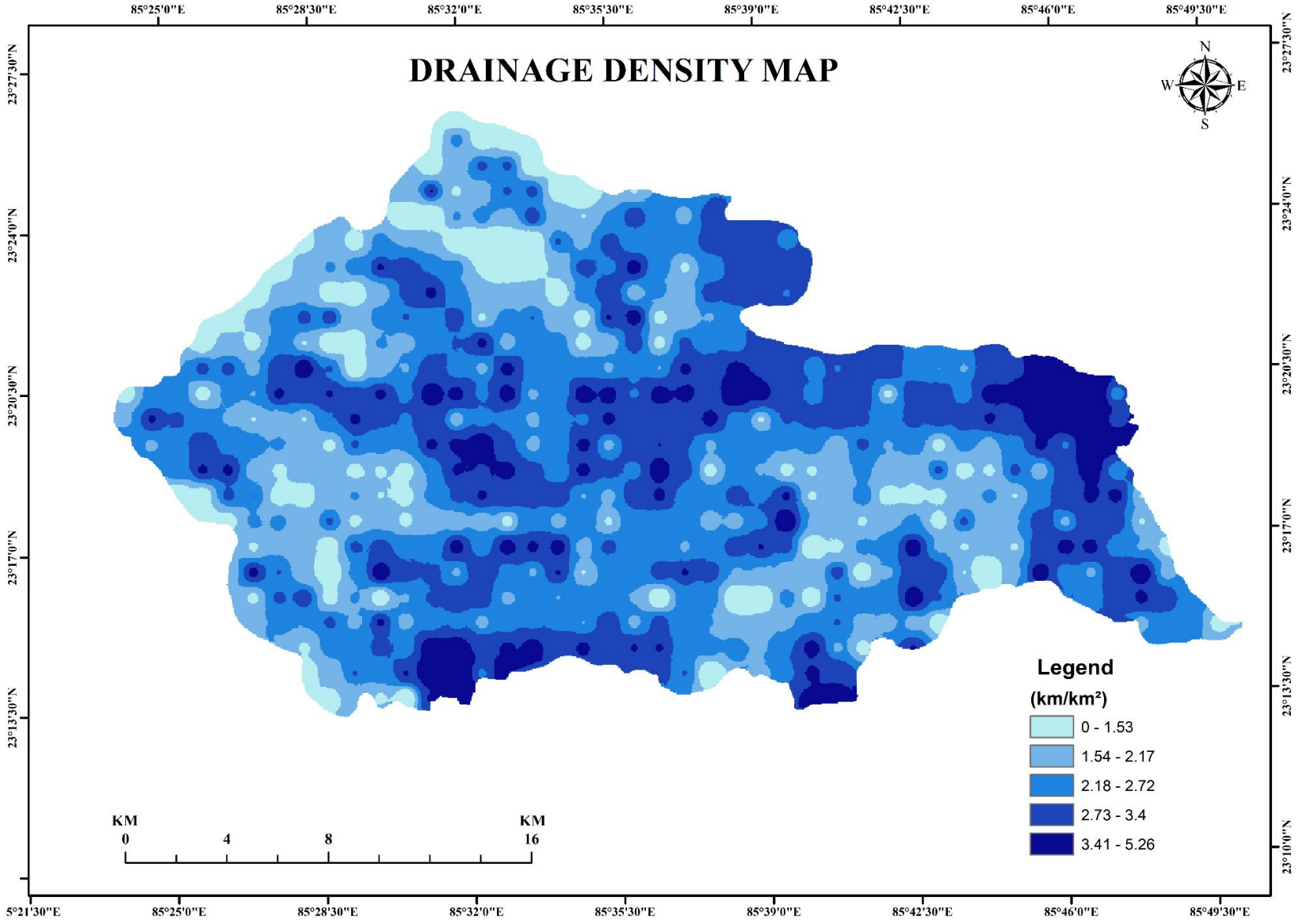
DRAINAGE DENSITY MAP
85°25'0"E
85°28'30"E
85°32'0"E
85°35'30"E
85°39'0"E
85°42'30"E
85°46'0"E
85°49'30"E
23°27'30"N
23°24'0"N
23°20'30"N
23°17'0"N
23°13'30"N
23°10'0"N
N
W
E
S
Legend
(km/km²)
0 - 1.53
1.54 - 2.17
2.18 - 2.72
2.73 - 3.4
3.41 - 5.26
KM
0
4
8
16
KM

Fig 8.Showing the Drainage density map of the study area.

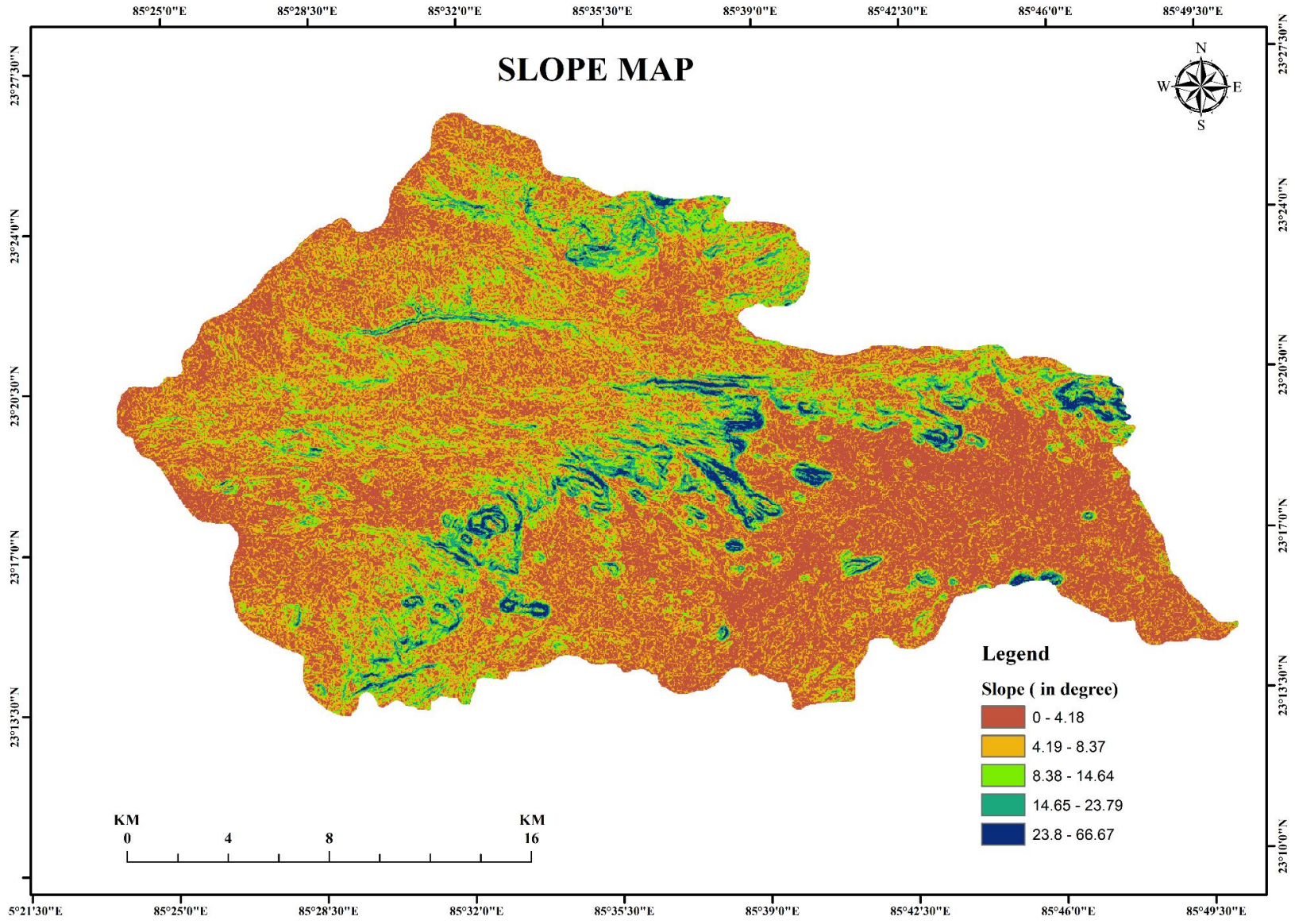
SLOPE MAP
85°25'0"E
85°28'30"E
85°32'0"E
85°35'30"E
85°39'0"E
85°42'30"E
85°46'0"E
85°49'30"E
23°27'30"N
23°24'0"N
23°20'30"N
23°17'0"N
23°13'30"N
23°10'0"N
N
W
E
S
Legend
Slope (in degree)
0 - 4.18
4.19 - 8.37
8.38 - 14.64
14.65 - 23.79
23.8 - 66.67
KM
0
4
8
16
KM

Fig 9. Showing the Slope map the study area.

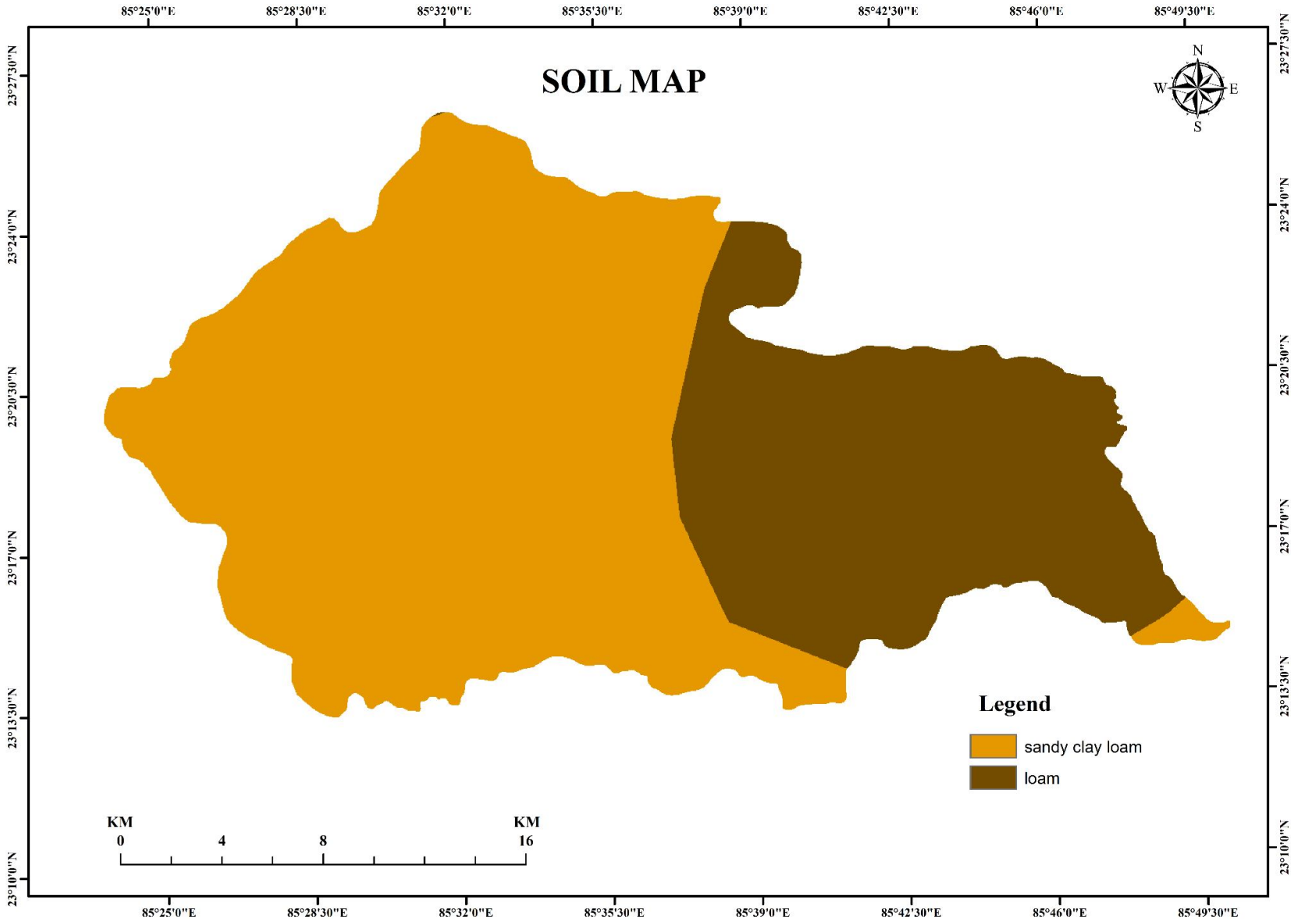
SOIL MAP
85°25'0"E
85°28'30"E
85°32'0"E
85°35'30"E
85°39'0"E
85°42'30"E
85°46'0"E
85°49'30"E
23°27'30"N
23°24'0"N
23°20'30"N
23°17'0"N
23°13'30"N
23°10'0"N
N
W
E
S
Legend
sandy clay loam
loam
KM
0
4
8
KM
16

Fig 10.Showing the Soil map the study area.

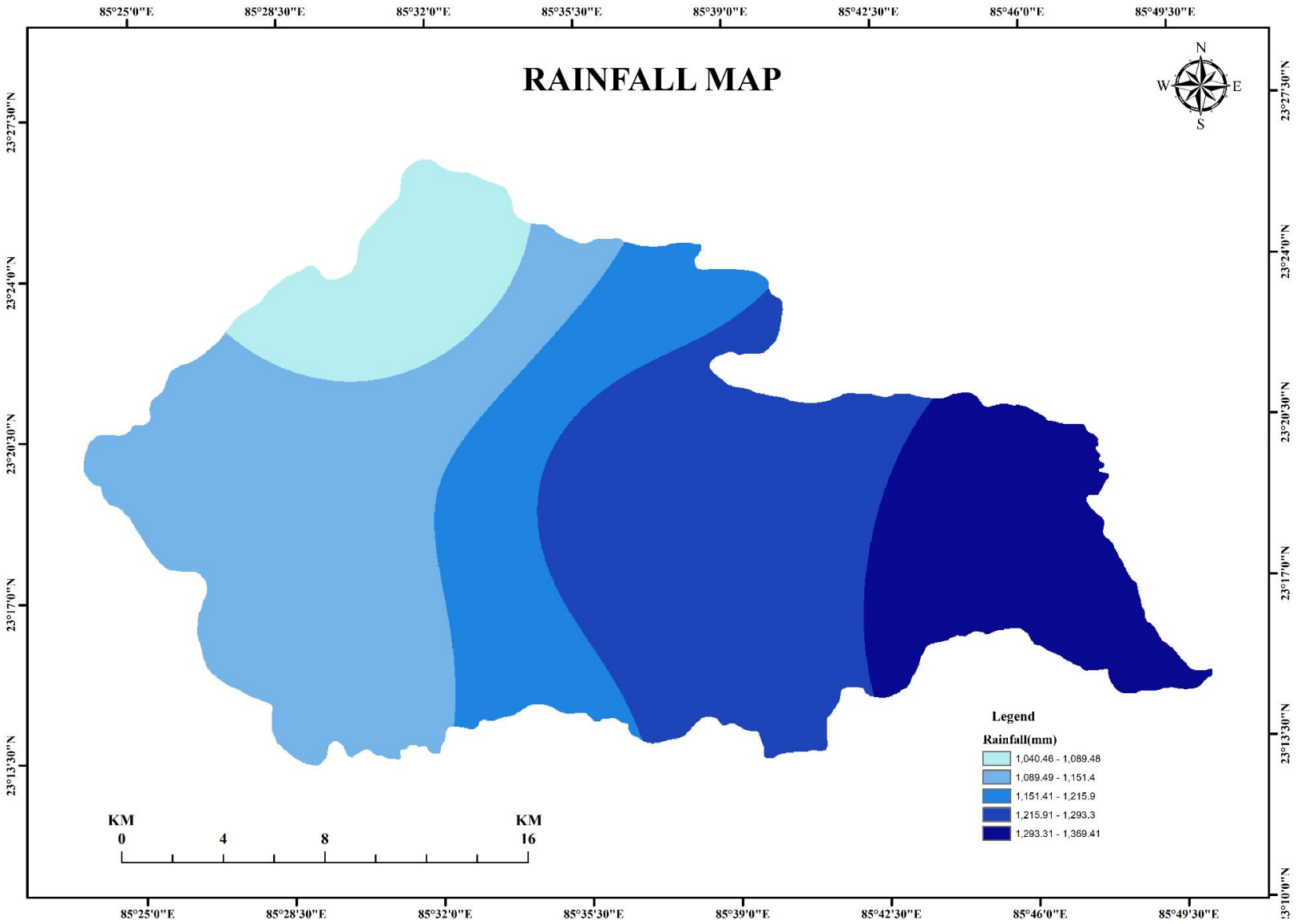
RAINFALL MAP
85°25'0"E
85°28'30"E
85°32'0"E
85°35'30"E
85°39'0"E
85°42'30"E
85°46'0"E
85°49'30"E
23°27'30"N
23°24'0"N
23°20'30"N
23°17'0"N
23°13'30"N
N
W
E
S
KM
0
4
8
16
Legend
Rainfall(mm)
1,040.46 - 1,089.48
1,089.49 - 1,151.4
1,151.41 - 1,215.9
1,215.91 - 1,293.3
1,293.31 - 1,369.41

Fig 11. Showing the Rainfall map the study area.

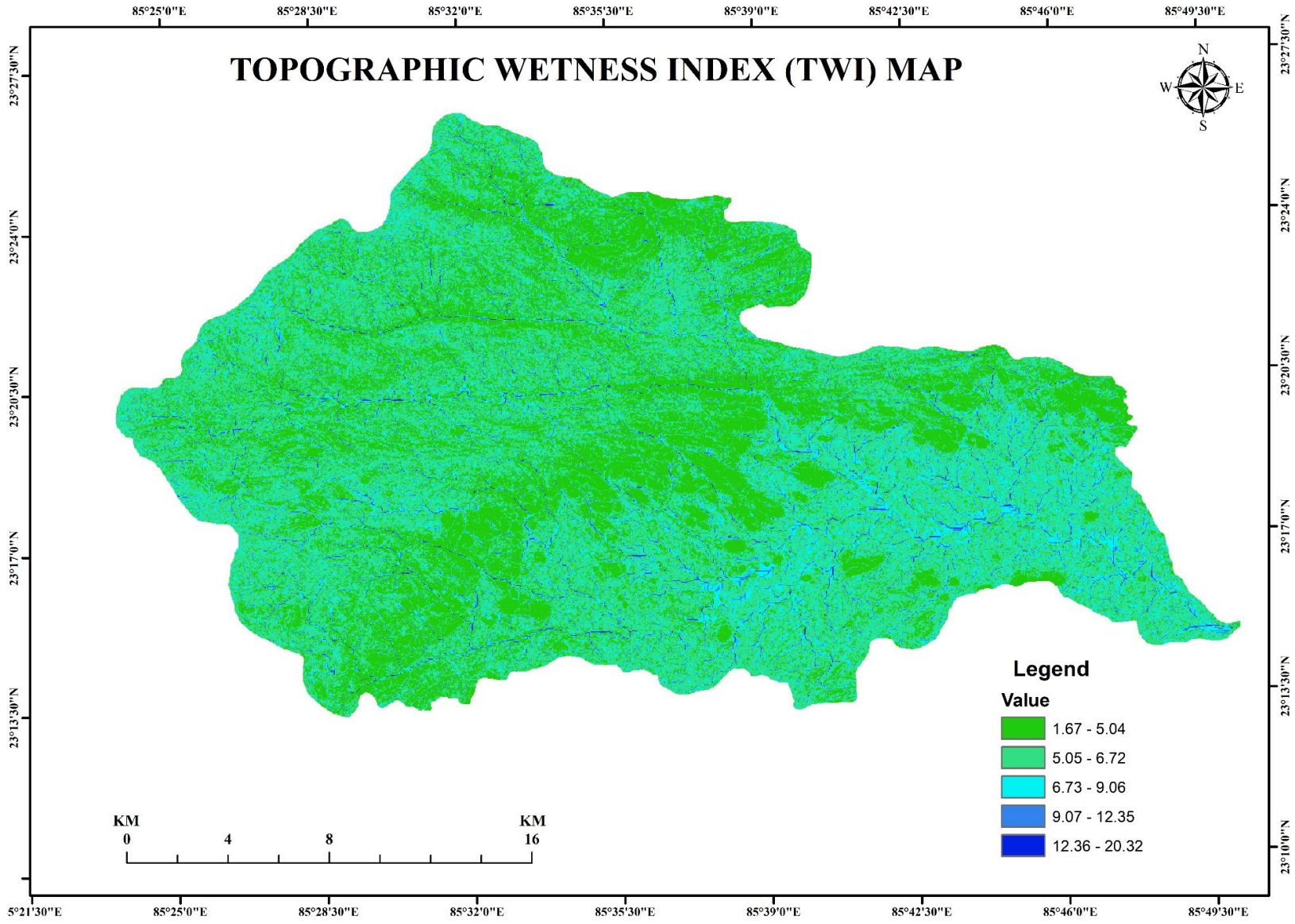
TOPOGRAPHIC WETNESS INDEX (TWI) MAP
N
W
E
S
85°25'0"E
85°28'30"E
85°32'0"E
85°35'30"E
85°39'0"E
85°42'30"E
85°46'0"E
85°49'30"E
23°27'30"N
23°24'0"N
23°20'30"N
23°17'0"N
23°13'30"N
23°10'0"N
Legend
Value
1.67 - 5.04
5.05 - 6.72
6.73 - 9.06
9.07 - 12.35
12.36 - 20.32
KM
0
4
8
16

Fig 12.Showing the TWI map the study area.

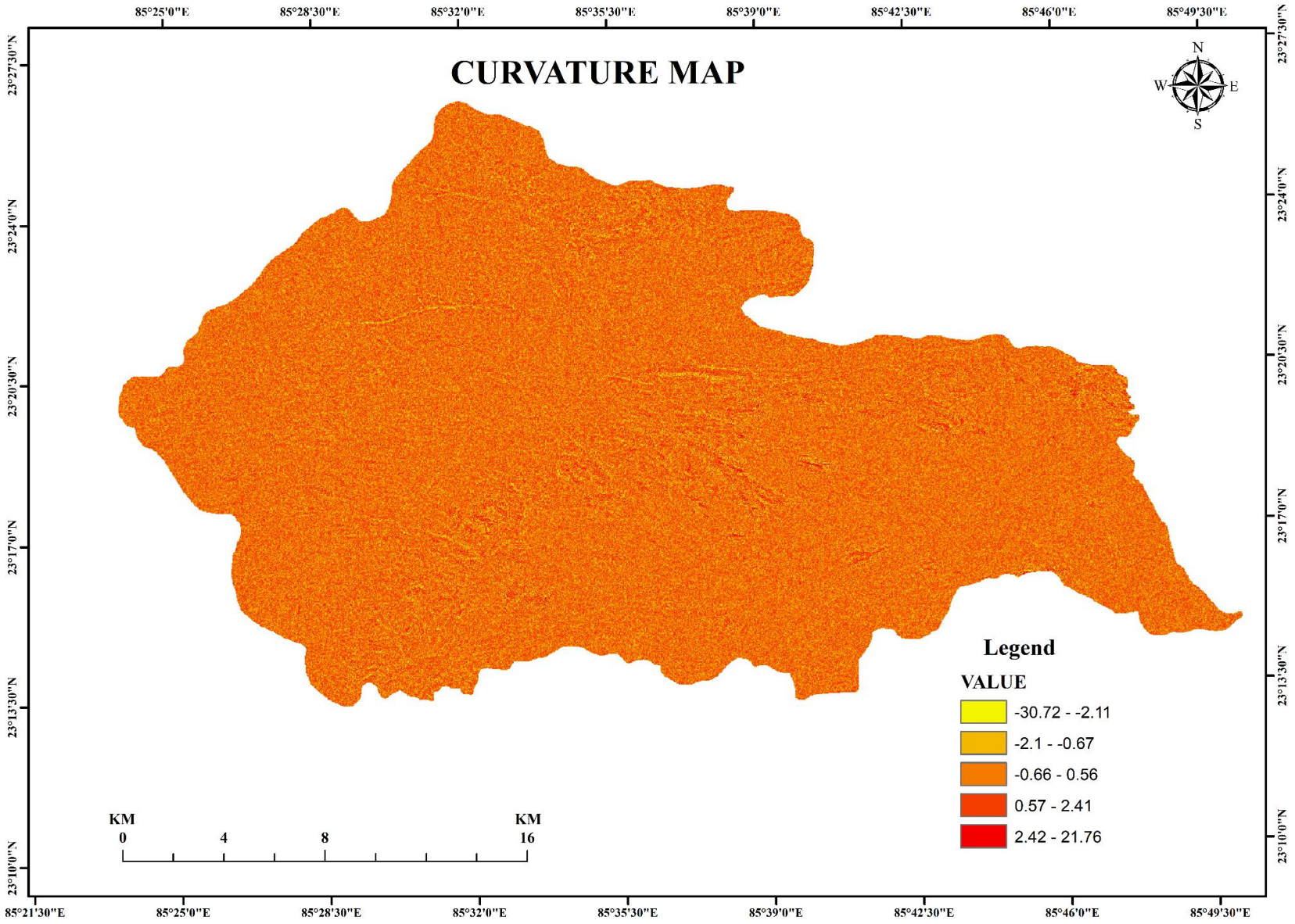
CURVATURE MAP
85°25'0"E
85°28'30"E
85°32'0"E
85°35'30"E
85°39'0"E
85°42'30"E
85°46'0"E
85°49'30"E
85°21'30"E
23°27'30"N
23°24'0"N
23°20'30"N
23°17'0"N
23°13'30"N
23°10'0"N
N
W
E
S
Legend
VALUE
-30.72 - -2.11
-2.1 - -0.67
-0.66 - 0.56
0.57 - 2.41
2.42 - 21.76
KM
0
4
8
KM
16

Fig 13. Showing the Curvature map the study area.

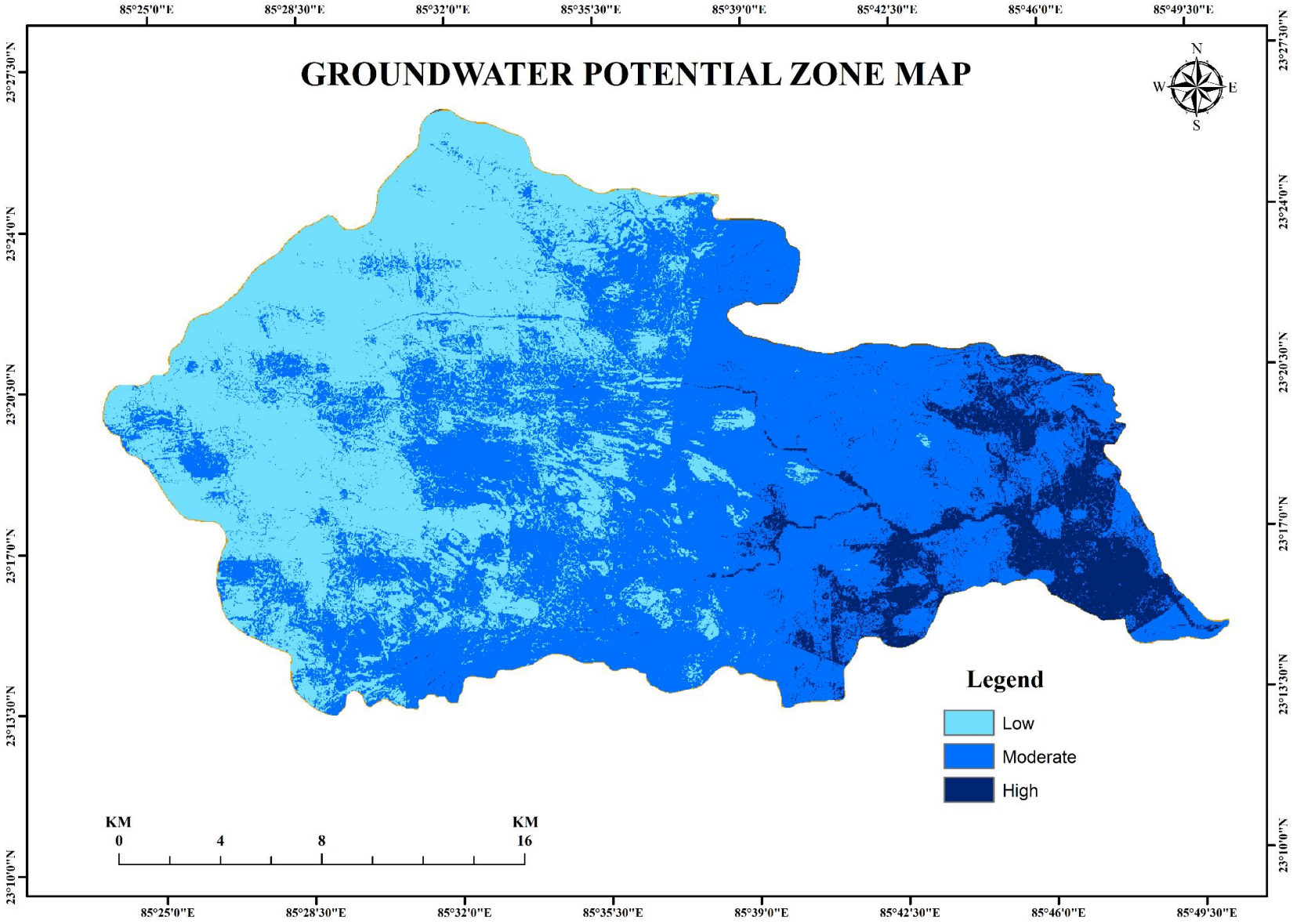
GROUNDWATER POTENTIAL ZONE MAP
N
W
E
S
85°25'0"E
85°28'30"E
85°32'0"E
85°35'30"E
85°39'0"E
85°42'30"E
85°46'0"E
85°49'30"E
23°27'30"N
23°24'0"N
23°20'30"N
23°17'0"N
23°13'30"N
23°10'0"N
Legend
Low
Moderate
High
KM
0
4
8
KM
16

Fig 14.Showing the Groundwater potential zone (GWPZ) map the study area.

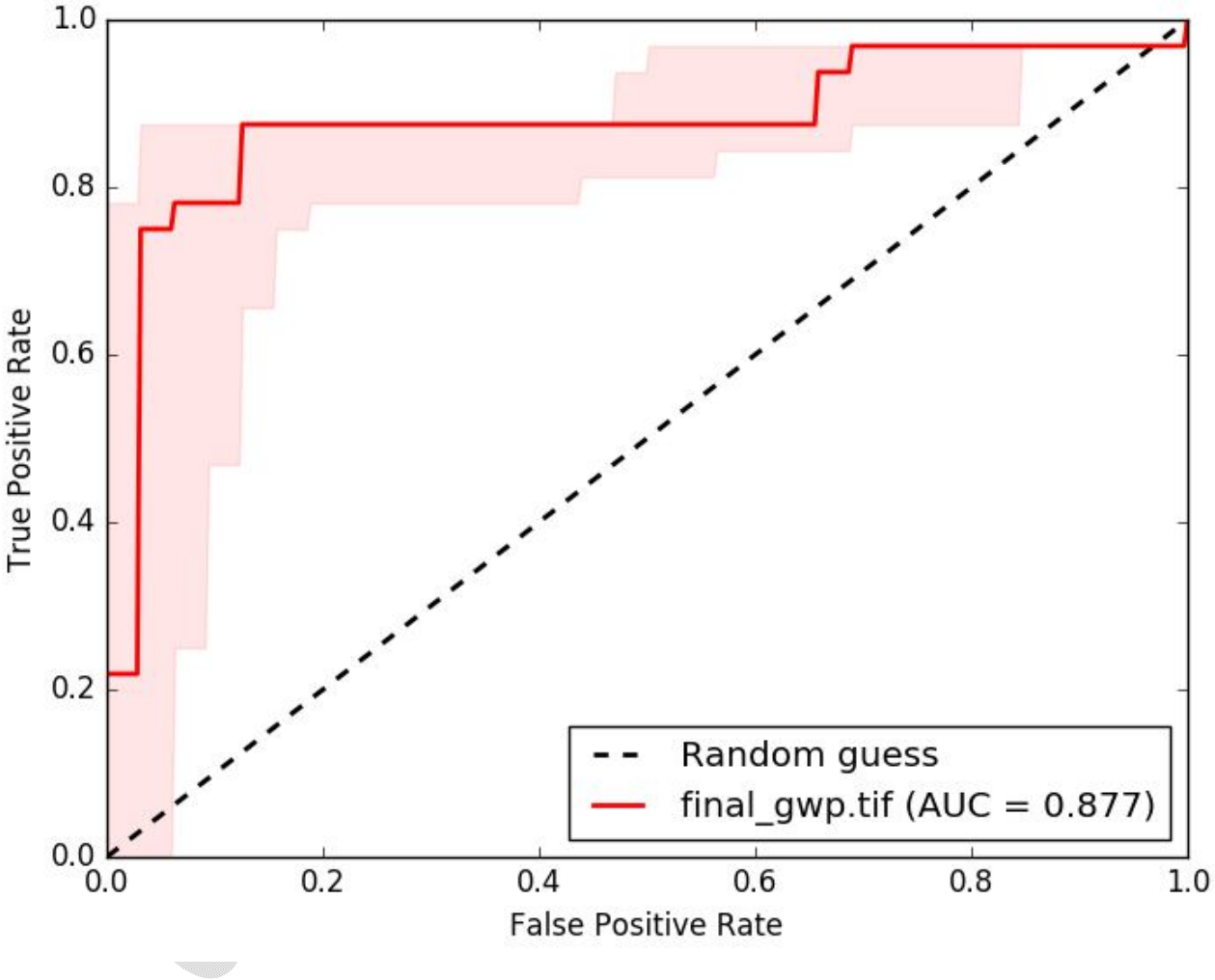
1.0
0.8
0.6
0.4
0.2
0.0
True Positive Rate
0.0
0.2
0.4
0.6
0.8
1.0
False Positive Rate
Random guess
final_gwp.tif (AUC = 0.877)

Fig 15. Showing Visual representation of the model validation results utilizing the Receiver Operating Characteristic (ROC) curve and the associated Area Under the Curve (AUC) metric.